

## Accepted Article

**Title:** Mono- and Bis-Imidazolidinium Ethynyl Cations and the Reduction of the Latter to give an Extended Bis-1,4-([3]Cumulene)-p-Carbo-Quinoid System

**Authors:** Brain Barry, Graeme Soper, Juha Hurmalainen, Akseli Mansikkamäki, Katherine N Robertson, William L McClennan, Alex J. Veinot, Tracey L. Roemmele, Ulrike Werner-Zwanziger, René T Boéré, Heikki M. Tuononen, Jason Clyburne, and Jason Masuda

This manuscript has been accepted after peer review and appears as an Accepted Article online prior to editing, proofing, and formal publication of the final Version of Record (VoR). This work is currently citable by using the Digital Object Identifier (DOI) given below. The VoR will be published online in Early View as soon as possible and may be different to this Accepted Article as a result of editing. Readers should obtain the VoR from the journal website shown below when it is published to ensure accuracy of information. The authors are responsible for the content of this Accepted Article.

**To be cited as:** *Angew. Chem. Int. Ed.* 10.1002/anie.201711031  
*Angew. Chem.* 10.1002/ange.201711031

**Link to VoR:** <http://dx.doi.org/10.1002/anie.201711031>  
<http://dx.doi.org/10.1002/ange.201711031>

## COMMUNICATION

# Mono- and Bis-Imidazolidinium Ethynyl Cations and the Reduction of the Latter to give an Extended Bis-1,4-([3]Cumulene)-*p*-Carbo-Quinoid System†

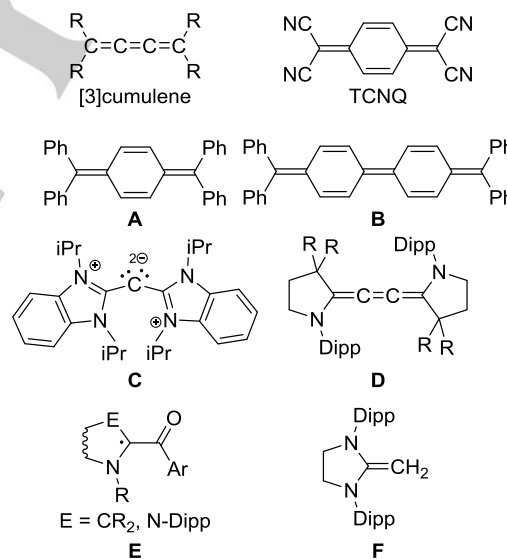
Brian M. Barry<sup>[a,b]</sup>, R. Graeme Soper<sup>[a]</sup>, Juha Hurmalainen<sup>[c]</sup>, Akseli Mansikkamäki<sup>[c]</sup>, Katherine N. Robertson<sup>[a]</sup>, William L. McClennan<sup>[a]</sup>, Alex J. Veinot<sup>[a]</sup>, Tracey L. Roemmele<sup>[d]</sup>, Ulrike Werner-Zwanziger<sup>[e]</sup>, René T. Boéré<sup>\*[d]</sup>, Heikki M. Tuononen<sup>\*[c]</sup>, Jason A. C. Clyburne<sup>\*[a]</sup>, Jason D. Masuda<sup>\*[a]</sup>

**Abstract:** An extended  $\pi$ -system containing two [3]cumulene fragments separated by a *p*-carbo-quinoid and stabilized by two capping *N*-heterocyclic carbenes (NHCs) has been prepared. Mono- and bis-imidazolidinium ethynyl cations have also been synthesized from the reaction of an NHC with phenylethynyl bromide or 1,4-bis(bromoethynyl)benzene. Cyclic voltammetry coupled with synthetic and structural studies showed that the dication is readily reduced to a neutral, singlet bis-1,4-([3]cumulene)-*p*-carbo-quinoid due to the  $\pi$ -accepting properties of the capping NHCs.

Extended cumulenes and polyynes have received much recent attention. For example, Tykwinski<sup>[1,2]</sup> and others<sup>[3]</sup> have used them as molecular wires and as linkers between the end caps of rotaxanes.<sup>[4]</sup> These extended linear carbon atom chains are conjugated  $\pi$ -systems, which allows for communication across their length.<sup>[2]</sup> Shorter cumulenes, such as [3]cumulenes, were first reported by Brand in the early 1920's.<sup>[5, 6]</sup> More recently, Diederich has looked at the synthesis and reactivity of these systems<sup>[7, 8]</sup> as well as those of a number of push-pull/donor-

acceptor [3]cumulenes.<sup>[9, 10]</sup> In addition, Ueta has reported the [2+2] cycloaddition of a [3]cumulene with tetracyanoethene.<sup>[11]</sup>

*Para*-carbo-quinoids are conjugated molecules with extended  $\pi$ -systems and, as such, are also of interest. However, stable *para*-carbo-quinoids are uncommon. A well-known exception is tetracyanoquinodimethane (TCNQ)<sup>[12]</sup>, which is commonly used in charge transfer salts and was influential in the development of organic electronics; the TTF·TCNQ complex<sup>[13-15]</sup> (TTF = tetrathiafulvalene) is considered to be the first organic metal. Also included in the category of *para*-carbo-quinoids are Thiele's **A**<sup>[16]</sup> and Tschitschibabin's<sup>[17]</sup> (Chichibabin's<sup>[18]</sup>) **B** hydrocarbons, both initially reported in the early 1900's. The stability of **A** and **B** is largely attributable to their four phenyl substituents (*cf.* cyano groups in TCNQ),<sup>[18]</sup> though compound **B** is highly oxygen sensitive as a consequence of its biradicaloid ground state.<sup>[19]</sup>



- [a] Prof. B. M. Barry, R. G. Soper, Dr. K. N. Robertson, A. J. Veinot, W. L. McClennan, Prof. J. A. C. Clyburne, Prof. J. D. Masuda  
Department of Chemistry  
Saint Mary's University  
Halifax, Nova Scotia, B3H 3C3 (Canada)  
E-mail: [jason.clyburne@smu.ca](mailto:jason.clyburne@smu.ca), [jason.masuda@smu.ca](mailto:jason.masuda@smu.ca)
- [b] Prof. B. M. Barry  
Department of Chemistry  
University of Wisconsin-Platteville  
Platteville, Wisconsin, 53818-3099 (USA)
- [c] J. Hurmalainen, A. Mansikkamäki, Prof. H. M. Tuononen  
Department of Chemistry, Nanoscience Centre  
University of Jyväskylä  
P.O. Box 35, University of Jyväskylä, FI-40014 (Finland)  
E-Mail: [heikki.m.tuononen@juu.fi](mailto:heikki.m.tuononen@juu.fi)
- [d] Dr. T. L. Roemmele, Prof. R. T. Boéré  
Department of Chemistry and Biochemistry  
University of Lethbridge  
Lethbridge, Alberta, T1K 3M4 (Canada)  
E-mail: [boere@uleth.ca](mailto:boere@uleth.ca)
- [e] Dr. U. Werner-Zwanziger  
Department of Chemistry  
Dalhousie University  
Halifax, Nova Scotia, B3H 4J3 (Canada)  
E-mail: [ulli.zwanziger@dal.ca](mailto:ulli.zwanziger@dal.ca)

† Part of this work was previously presented: R. G. Soper, B. M. Barry, W. L. McClennan, K. N. Robertson, J. Hurmalainen, T. L. Roemmele, H. M. Tuononen, R. T. Boéré, J. D. Masuda, J. A. C. Clyburne, *Mono- and bis-phenylpropargyl imidazolidinium cations: Structure and reduction behavior*. **2015**, 247<sup>th</sup> ACS National Meeting, Denver, Colorado, March 22-26, 2015.

Supporting information for this article is given via a link at the end of the document.

Unique main group functionalities can be stabilized using singlet carbenes of which *N*-heterocyclic carbenes (NHCs)<sup>[20]</sup> and cyclic alkyl amino carbenes (CAACs) are the most often employed.<sup>[21, 22]</sup> In terms of carbon-based functional groups, these singlet carbenes have been used to isolate bent allenes **C**<sup>[23]</sup>, (also formulated as NHC→C←NHC carbones)<sup>[24]</sup> and CAAC-functionalized [3]cumulenes **D**, including their dication and radical mono cations in which much of the spin density is carbon-based.<sup>[25-28]</sup> A [3]cumulene stabilized by two capping 4-pyridylidene units has also been reported.<sup>[29]</sup> In a similar vein, though carbene-centered radicals stabilized via the so-called captodative effect have been known for quite some time<sup>[30, 31]</sup>, stable NHC- and CAAC-based derivatives **E** have only recently

## COMMUNICATION

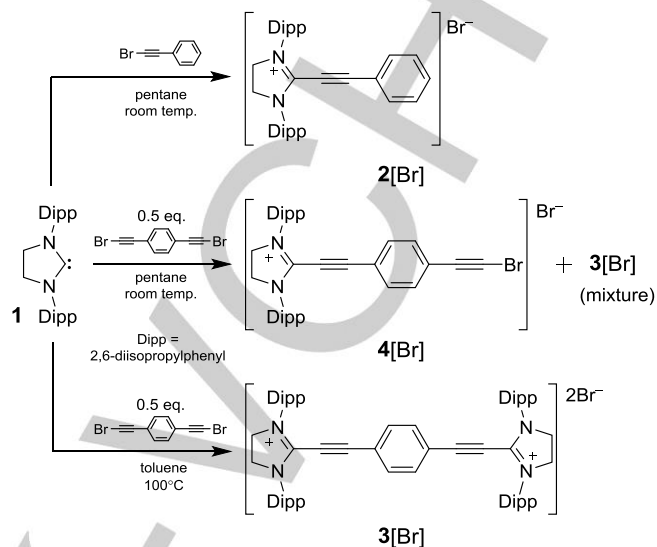
been reported by Bertrand<sup>[32, 33]</sup> and Hudnall.<sup>[34]</sup> Finally, it would be remiss to not mention the recent work of Rivard on *N*-heterocyclic olefins **F**<sup>[35]</sup> which are isolable molecules prepared from the reaction of an NHC and (Me<sub>3</sub>Si)CH<sub>2</sub>Cl.<sup>[36]</sup>

Here we report the chemistry of the NHC, 1,3-bis(2,6-diisopropylphenyl)imidazolidin-2-ylidene **1**, with ethynyl halides, further expanding the reactivity of NHCs with carbon-based functional groups. Specifically, we describe the synthesis of mono- and bis-imidazolium ethynyl cation-based salts **2**[Br] and **3**[Br], both propargyl cations, which have been characterized by a variety of structural methods, including spectroscopy, X-ray diffraction, and comparative computational studies. The redox chemistry of the cations **2** and **3** has also been explored and in the case of **3**, a double reduction was found to give a neutral, singlet bis-1,4-([3]cumulene)-*p*-carbo-quinoid **5**. The isolation of **5** can be attributed to the  $\pi$ -accepting properties of the NHC working in conjunction with the ability of the 1,4-ethynyl benzene group to readily reorganize to form the bis-1,4-([3]cumulene)-*p*-carbo-quinoid containing a total of 24  $\pi$ -electrons (including the *N*-based lone pairs). This is in contrast to a recent computational study where derivatives that lack substantial  $\pi$ -accepting properties (e.g. carbene, R<sub>2</sub>C, R = alkyl, aryl, nitrile, acetylene), form biradical species that maintain the non-quinoidal, -C $\equiv$ C-C<sub>6</sub>H<sub>4</sub>-C $\equiv$ C- bonding pattern.<sup>[37]</sup>

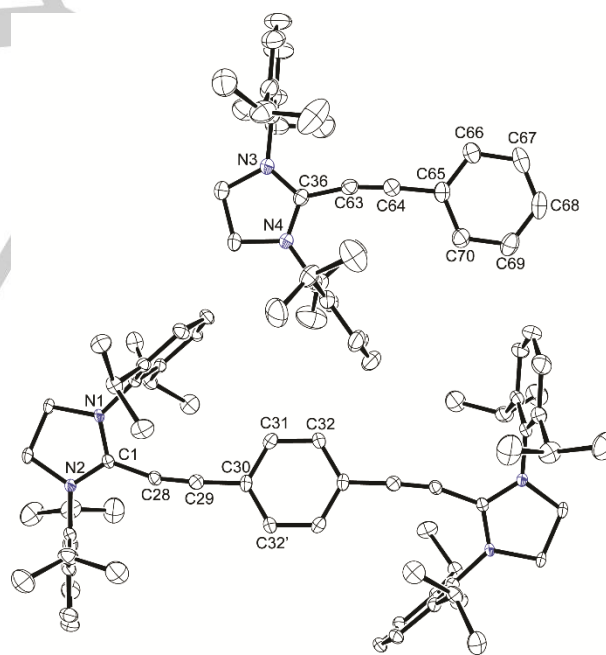
NHC **1** readily reacts with phenylethynyl bromide at room temperature in pentane to give the salt **2**[Br] in reasonable yield (57%) as a tan colored powder (Scheme 1). However, the reaction of NHC **1** with 1,4-bis(bromoethynyl)benzene did not go to completion at room temperature (Scheme 1). Even with extended stirring, mixtures of **3**[Br] were contaminated with compound **4**[Br] (1:0.6 ratio by <sup>1</sup>H NMR spectroscopy), most likely due to the insolubility of **4**[Br] in pentane preventing further reaction with NHC **1**. Alternatively, reacting **1** with 1,4-bis(bromoethynyl)benzene in hot (100°C) toluene overnight gave **3**[Br] as the only product in high isolated yield (89%). Compounds **2**[Br] and **3**[Br] were characterized by elemental analysis, IR, <sup>1</sup>H, and <sup>13</sup>C NMR spectroscopies, and single crystal X-ray diffraction (Figure 1), whereas the impurity **4** was characterized (as its BPh<sub>4</sub> salt) by X-ray crystallography (see Supporting Information).

IR and <sup>13</sup>C NMR spectroscopies clearly identified the ethyne groups in **2** and **3** (**2**:  $\nu = 2223\text{ cm}^{-1}$ ,  $\delta = 72.4$  and  $110.4\text{ ppm}$ ; **3**:  $\nu = 2227\text{ cm}^{-1}$ ,  $\delta = 75.0$  and  $109.8\text{ ppm}$ ). In the solid state (Figure 1), both **2** and **3** feature typical C<sub>NHC</sub>-C<sub>alkynyl</sub> (**2**: 1.423(4) and 1.424(4) Å; **3**: 1.417(4) Å)<sup>[38]</sup> and C $\equiv$ C bond lengths (**2**: 1.196(4) and 1.203(4) Å; **3**: 1.197(4) Å). In addition, the C<sub>NHC</sub>-C $\equiv$ C angle is nearly linear in one of the two crystallographically inequivalent cations in **2**[Br] (171.3(3)°), slightly more bent in the second (167.3(3)°), and considerably bent (163.9(3)°) in the dication **3**. Density Functional Theory (DFT) calculations (PBE1PBE<sup>[39-42]</sup>/(def2-)TZVP<sup>[43,44]</sup>) on the cations **2** and **3** showed that a linear C<sub>NHC</sub>-C $\equiv$ C-C arrangement is preferred, implying that the observed bending is most likely a crystal packing effect due to a shallow potential for angle bending (see Supporting Information). This was confirmed by synthesizing a number of other mono-cation compounds similar to **2**, which were characterized using X-ray diffraction (**2**[PF<sub>6</sub>], *para*-F-**2**[PF<sub>6</sub>], *para*-Ph-**2**[Br]); see Supporting Information). An analysis of bond lengths and angles for the C<sub>NHC</sub>-C $\equiv$ C-Ar portion of the cations gave significant variation in the C<sub>NHC</sub>-C $\equiv$ C bond angle (from 163.9(3)° to 180.0°), showing that

this is indeed the one position in each compound where flexibility can be induced during packing for crystallization. Finally, it should be noted that the C-C bond distances in the aryl ring attached to the acetylene are consistent with those in a normal aromatic ring (**2**: 1.348(9)–1.415(6) Å; **3**: 1.386(4)–1.399(5) Å).



**Scheme 1.** Synthetic route to compounds **2**[Br], **3**[Br], and **4**[Br], from NHC **1** and ethynyl bromides.



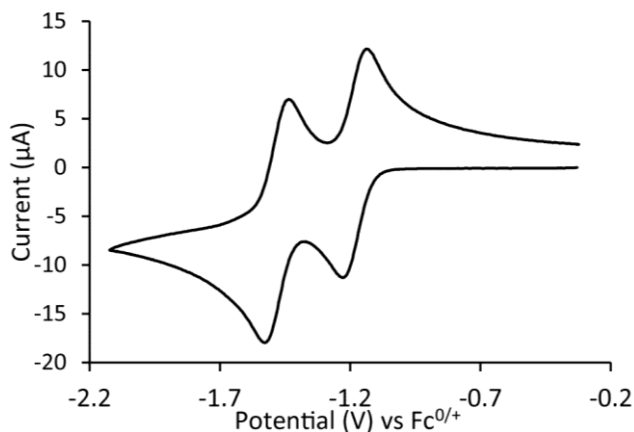
**Figure 1.** Solid state structure of the cation **2** (top, one of two cations in the asymmetric unit) and the dication **3** (bottom). Hydrogen atoms, anions, and co-crystallized solvent molecules have been omitted for clarity.

Compounds **2**[Br] and **3**[Br] were analyzed by cyclic voltammetry. The reduction of **2**[Br] was found to be a scan-rate dependent process, whereby the anodic peak current increased upon faster scanning ( $\nu = 0.2\text{--}20\text{ V s}^{-1}$ ) ( $E_m = -1.63\text{V vs Fc}^{0/+}$ ). No processes were observed upon initial scanning in the anodic direction to 0 V. However, upon scanning first in the cathodic

## COMMUNICATION

direction an induced process was observed at  $E = -0.73$  V vs  $\text{Fc}^{0/+}$  (see Supporting Information). The peak current for this process was small and *decreased* with increasing scan rate (such a peak was not observed in scans greater than  $10 \text{ V s}^{-1}$ ; see Supporting Information). Attempts to chemically reduce the cation ( $\text{KC}_8$ ) resulted in a dark red colored intractable material that gave a weak EPR signal. Multiple attempts to obtain pure material were unsuccessful and attempts to further identify this product were abandoned. DFT calculations showed that the unpaired electron in the purported neutral radical is highly delocalized. This does not, however, preclude the possibility for C-C bond formation via the terminal phenyl group.

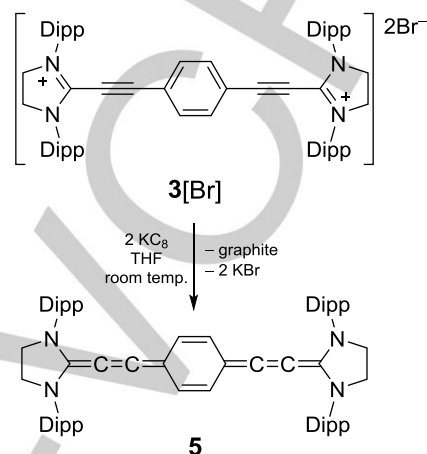
Compound **3** was found to undergo two sequential, reversible redox processes (*i.e.* an  $E_{\text{rev}}E_{\text{rev}}$  mechanism<sup>[45]</sup>) with  $E_m$  of  $-1.18$  V and  $-1.48$  V vs  $\text{Fc}^{0/+}$  (Figure 2). The first process is likely a one electron reduction to form a radical cation, followed by a second reduction to give the neutral species.<sup>[46]</sup> These redox processes are much lower in potential than those of TCNQ ( $-0.30$  V and  $-0.88$  V vs  $\text{Fc}^{0/+}$ ).<sup>[47]</sup> Chemical reduction of **3**[Br] with two equivalents of  $\text{KC}_8$  in THF resulted in rapid formation of an intensely blue colored solution with black precipitate (graphite). Upon workup, a blue-black material was obtained in low isolated yield (33%) due to its extreme solubility in compatible solvents (pentane, toluene, or THF). IR spectroscopy showed the introduction of a new signal at  $2082 \text{ cm}^{-1}$ , and the concomitant loss of the  $\text{C}\equiv\text{C}$  stretch ( $\nu = 2227 \text{ cm}^{-1}$  in **3**[Br]), which is consistent with the presence of a cumulene functional group and the formation of **5** (Scheme 2).



**Figure 2.** Cyclic voltammogram of compound **3**[Br] in  $\text{CH}_2\text{Cl}_2$  containing  $0.4 \text{ M}$   $[\text{Bu}_4\text{N}][\text{PF}_6]$  at a Pt electrode at room temperature; sweep rate  $0.2 \text{ V s}^{-1}$  with the potential starting at  $-0.3$  V and sweeping in the anodic direction first.

The neutral reduction product **5** could conceivably exist in any of three possible forms: a neutral open shell biradical (singlet or triplet) or as a neutral closed shell singlet cumulene.<sup>[18]</sup> DFT calculations indicated that the closed shell singlet form is the global energy minimum and lies *ca.*  $60 \text{ kJ mol}^{-1}$  below the open shell triplet biradical state; there was no indication of a low-energy open shell singlet state. Magnetic susceptibility measurements on the solid confirmed that **5** is diamagnetic and carefully prepared samples were EPR silent. Although a clean solution state  $^1\text{H}$  NMR spectrum of **5** could not be obtained, most likely due to the presence of very minor amounts of paramagnetic impurities, a clean solid state  $^{13}\text{C}$  NMR spectrum was recorded and showed

good correlation with the calculated chemical shifts (see Supporting Information). The solution UV-Vis spectrum for **5** showed one main absorption at  $595 \text{ nm}$  (pentane,  $\epsilon = 23970 \text{ L mol}^{-1} \text{ cm}^{-1}$ ), which matches with the observed blue color of the solution. The calculated  $\lambda_{\text{max}}$  of **5** is *ca.*  $550 \text{ nm}$  in *n*-pentane ( $525 \text{ nm}$  in gas phase), which is reasonably close to the observed main absorption and corresponds to a HOMO to LUMO transition with no charge transfer character (see Supporting Information).

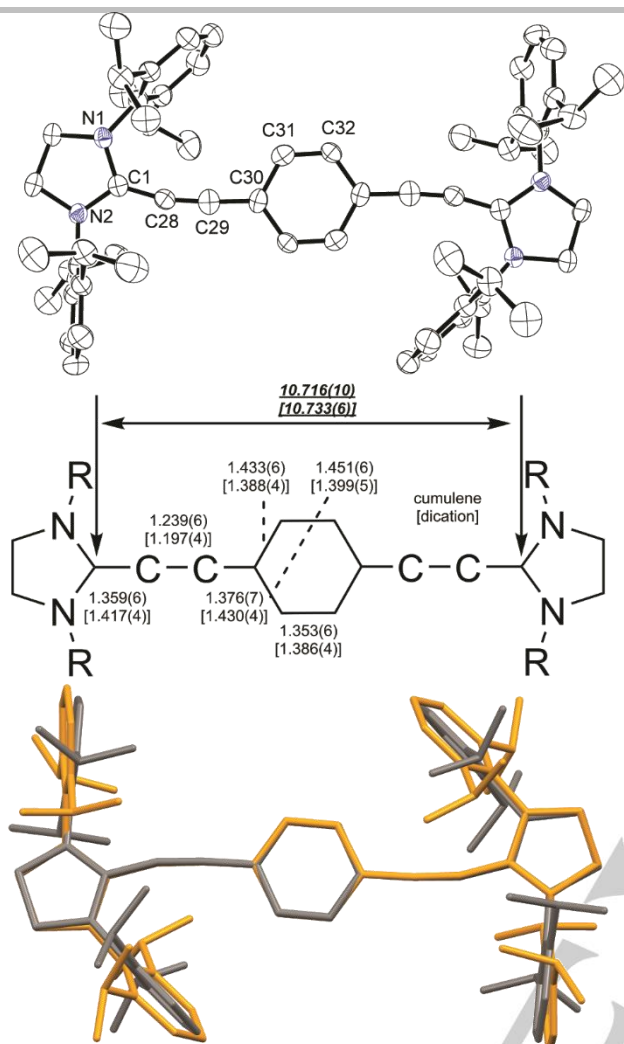


**Scheme 2.** Reduction of **3**[Br] to form the cumulene **5**.

Dark blue/black crystals of **5** were grown from a cold ( $-35^\circ\text{C}$ ) pentane solution and were found to be suitable for analysis by X-ray crystallography (Figure 3, top). Compound **5** crystallizes in the space group  $P2_1/c$  with the asymmetric unit containing one-half of the molecule. The metrical parameters for **5** are significantly different from **3** in each of the bond lengths between the two NHC fragments (Figure 3, middle). The  $\text{C}_{\text{NHC}}\text{-C}$  bond is shorter by *ca.* 4%, while the central C-C bond has elongated by *ca.* 3.5% (*i.e.* no longer  $\text{C}\equiv\text{C}$ ) and the  $\text{C-C}_6\text{H}_4\text{-C}$  fragment has distinct quinoidal character with alternating double and single bonds. Fascinatingly, both the dication **3** and the cumulene **5** have nearly identical *overall* structures (see the overlay in Figure 3, bottom). Thus, the addition of two electrons to **3** to afford **5** causes no perceptible change in the separation of the  $\text{NHC}\cdots\text{NHC}$  moieties in these species (**3**  $10.733(6) \text{ \AA}$  and **5**  $10.716(10) \text{ \AA}$ ) as a result of the offsetting C-C bond lengthening and shortening in the central  $(\text{CC})\text{C}_6\text{H}_4(\text{CC})$  core.

Bond length alternation (BLA) in cumulenes was originally observed by Tykwinski<sup>[48]</sup> using X-ray crystallographic data. It has been noted that BLA is greatest with [3]cumulenes and decreases as the cumulene chain lengthens. Cumulene **5** has a BLA of  $0.085$ .<sup>[49]</sup> When compared to other [3]cumulenes, **5** has a BLA that is similar to a standard cumulene ( $\text{R}_2\text{C}=\text{C}=\text{C}=\text{CR}_2$ ,  $\text{R} = 3,5\text{-}t\text{BuPh}$ ;  $\text{BLA} = 0.086$ ) and much different than that of a polarized [3]cumulene,  $((\text{Ph}(i\text{Pr})\text{N})(\text{Ph}(\text{Me})\text{N})\text{C}=\text{C}=\text{C}(\text{CN})_2)$ ;  $\text{BLA} = 0.172$ ), which reflects the relatively symmetrical nature of each [3]cumulene in **5**. The  $\text{C}_{\text{NHC}}\text{-C}=\text{C}$  angle ( $167.0(5)^\circ$ ) is slightly less bent than that in the dicationic precursor ( $163.9(3)^\circ$ ). However, a computational analysis of **5** showed that a linear  $\text{C}_{\text{NHC}}\text{-C}\equiv\text{C}$  arrangement is again preferred in the gas phase with a shallow potential for angle bending (see Supporting Information).


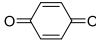
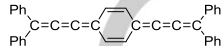
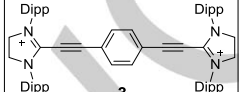
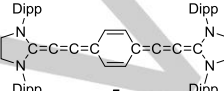
## COMMUNICATION



**Figure 3.** Solid state structure of cumulene **5** (top; 50% ellipsoids, hydrogen atoms removed), bond lengths (Å) of cumulene **5** and dication **3** [in brackets] (middle), and an overlay of both the dication **3** (grey) and cumulene **5** (orange) showing the similarity between the structures (bottom).

Nucleus Independent Chemical Shift (NICS) calculations were performed for **5** and the results were compared to values calculated for the dication **3** as well as to those of three model systems: benzene, *p*-benzoquinone, and a phenyl substituted [3]cumulene similar to **5**.<sup>[50]</sup> The results (Table 1) show that the central ring in **3** has a NICS(1)<sub>zz</sub> value quite similar to that of benzene (-24 ppm and -30 ppm, respectively), indicative of aromatic character, whereas the cumulene **5** has a NICS(1)<sub>zz</sub> value very similar to that calculated for *p*-benzoquinone (2 ppm and 3 ppm, respectively), consistent with their antiaromatic nature. This data, along with the bond lengths from the crystal structures, reinforces the idea that there is a loss of aromaticity at the central C<sub>6</sub>H<sub>4</sub> ring when the dication of **3** is converted to the cumulene **5**, and supports the quinoidal description of the central ring in **5**. The quinoidal description of **5** is also supported by the morphology of the HOMO (*i.e.* the LUMO of the dication **3**), which shows alternating bonding/anti-bonding character for the C-C bonds of the central ring (see Supporting Information).

**Table 1.** Calculated Nucleus Independent Chemical Shifts

Compound	NICS(1) <sub>zz</sub> (ppm)
	-30
	3
	-6
	-24
	2

In conclusion, we have shown that NHCs react with ethynyl bromides to give mono- and bis-imidazolidinium ethynyl cations. Although the mono cation **2** produces intractable materials upon chemical reduction, the bis-substituted dication **3** can be reduced to give a novel bis-cumulene **5** that is quinoidal in character, as evidenced by X-ray crystallography and DFT calculations. We also discovered that there is very little change in the distance between the NHC moieties upon adding two electrons to the dication **3** to form **5**. This may prove to have useful applications in materials chemistry where disruption of the solid state structure is to be avoided, *e.g.* crystalline redox switches.

While readying this manuscript for submission, we discovered the recent pre-publication of the first crystalline monomeric allenyl/propargyl radical stabilized by CAAC ligands by the Bertrand group.<sup>[51]</sup> This communication highlights the significance and currency of the results reported herein. Rapid advances in the chemistry of carbon species enabled and supported by singlet carbenes can be expected.

As recommended by a reviewer, we attempted the reaction of **5** dissolved in degassed C<sub>6</sub>D<sub>6</sub> with one atmosphere of dihydrogen and noted no reaction at room temperature. Despite the small singlet-triplet energy gap of **5**, the morphologies of its frontier orbitals are not suitable for this type of reactivity. However, compound **5** is extremely reactive towards CH<sub>2</sub>Cl<sub>2</sub> and CHCl<sub>3</sub>, resulting in loss of its blue color in such solutions. The reaction products were not characterized.

## Experimental Section

See Supporting Information for experimental, computational, and extended crystallographic details. CCDC 1549498-1549504 contain the supplementary crystallographic data. These data can be obtained free of charge from the Cambridge Crystallographic Database Centre.

## COMMUNICATION

## Acknowledgements

JDM, JACC, and RTB acknowledge the support of individual Discovery Grants from the Natural Sciences and Engineering Research Council as well as individual funding from the Canadian Foundation for Innovation, the Nova Scotia Research and Innovation Trust (JDM, JACC), and the Government of Alberta (RTB). JACC is thankful to the Government of Canada for a Canada Research Chair. HMT, AM, and JH acknowledge financial support from the University of Jyväskylä and Emil Aaltonen foundation as well as computational resources provided by CSC – IT Centre for Science and the Finnish Grid and Cloud Infrastructure (persistent identifier urn:nbn:fi:research-infras-2016072533). UW-Z acknowledges support from the NMR-3 facility at Dalhousie University. Michel B. Johnson is acknowledged for collecting the magnetic susceptibility data.

**Keywords:** cumulenes • *N*-heterocyclic carbenes • alkynes • X-ray crystallography • propargyl cations

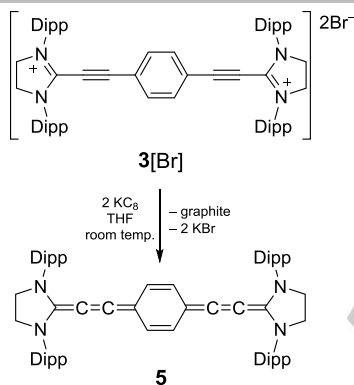
- [1] R. R. Tykwinski, *Chem. Rec.* **2015**, *15*, 1060-1074.
- [2] C. S. Casari, M. Tommasini, R. R. Tykwinski, A. Milani, *Nanoscale* **2016**, *8*, 4414-4435.
- [3] F. F. Diederich, M. Kivala, *Adv. Mater.* **2010**, *22*, 803-812.
- [4] D. Prenzel, R. R. Tykwinski in *Synthetic Methods for Conjugated Polymer and Carbon Materials*, (Eds. M. Leclerc, J.-F. Morin), Wiley-VCH, Weinheim, **2017**, pp. 255-291.
- [5] K. Brand, F. Kercher, *Ber. Dtsch. Chem. Ges. (A and B Series)* **1921**, *54*, 2007-2017.
- [6] K. Brand, *Ber. Dtsch. Chem. Ges. (A and B Series)* **1921**, *54*, 1987-2006.
- [7] P. Gawel, C. Dengiz, A. D. Finke, N. Trapp, C. Boudon, J. Gisselbrecht, F. Diederich, *Angew. Chem. Int. Ed.* **2014**, *53*, 4341-4345; *Angew. Chem.* **2014**, *126*, 4430-4434.
- [8] J. van Loon, P. Seiler, F. Diederich, *Angew. Chem. Int. Ed. Engl.* **1993**, *32*, 1187-1189; *Angew. Chem.* **1993**, *105*, 1235-1238.
- [9] Y. Wu, F. Tancini, W. B. Schweizer, D. Paunescu, C. Boudon, J. Gisselbrecht, P. D. Jarowski, E. Dalcanale, F. Diederich, *Chem. Asian J.* **2012**, *7*, 1185-1190.
- [10] P. Gawel, Y. Wu, A. D. Finke, N. Trapp, M. Zalibera, C. Boudon, J. Gisselbrecht, W. B. Schweizer, G. Gescheidt, F. Diederich, *Chem. Eur. J.* **2015**, *21*, 6215-6225.
- [11] S. Ueta, K. Hida, M. Nishiuchi, Y. Kawamura, *Org. Biomol. Chem.* **2014**, *12*, 2784-2791.
- [12] D. S. Acker, W. R. Hertler, *J. Am. Chem. Soc.* **1962**, *84*, 3370-3374.
- [13] L. B. Coleman, M. J. Cohen, D. J. Sandman, F. G. Yamagishi, A. F. Garito, A. J. Heeger, *Solid State Commun.* **1973**, *12*, 1125-1132.
- [14] J. Ferraris, D. O. Cowan, V. Walatka, J. H. Perlstein, *J. Am. Chem. Soc.* **1973**, *95*, 948-949.
- [15] M. J. Cohen, L. B. Coleman, A. F. Garito, A. J. Heeger, *Phys. Rev. B* **1974**, *10*, 1298-1307.
- [16] J. Thiele, H. Balhorn, *Ber. Dtsch. Chem. Ges.* **1904**, *37*, 1463-1470.
- [17] A. E. Tschitschibabin, *Ber. Dtsch. Chem. Ges.* **1907**, *40*, 1810-1819.
- [18] L. K. Montgomery, J. C. Huffman, E. A. Jurczak, M. P. Grendze, *J. Am. Chem. Soc.* **1986**, *108*, 6004-6011.
- [19] P. Ravat, M. Baumgarten, *Phys. Chem. Chem. Phys.* **2015**, *17*, 983-991.
- [20] L. J. Murphy, K. N. Robertson, J. D. Masuda, J. A. C. Clyburne in *N-Heterocyclic Carbenes: Effective Tools for Organometallic Synthesis*, (Ed. S.P. Nolan), Wiley-VCH, Weinheim, **2014**, 427-498.
- [21] M. Melaimi, R. Jazzar, M. Siolihavoup, G. Bertrand, *Angew. Chem. Int. Ed.* **2017**, *56*, 10046; *Angew. Chem.* **2017**, *129*, 10180-10203.
- [22] M. Soleilhavoup, G. Bertrand, *Acc. Chem. Res.* **2015**, *48*, 256-266.
- [23] C. Dyker, V. Lavallo, B. Donnadiéu, G. Bertrand, *Angew. Chem. Int. Ed.* **2008**, *47*, 3206-3209; *Angew. Chem.* **2008**, *120*, 3250-3253.
- [24] S. Klein, R. Tonner, G. Frenking, *Chem. Eur. J.* **2010**, *16*, 10160-10170.
- [25] Y. Li, K. C. Mondal, P. P. Samuel, H. Zhu, C. M. Orben, S. Panneerselvam, B. Dittrich, B. Schwederski, W. Kaim, T. Mondal, D. Koley, H. W. Roesky, *Angew. Chem. Int. Ed.* **2014**, *53*, 4168-4172; *Angew. Chem.* **2014**, *126*, 4252-4256.
- [26] L. Jin, M. Melaimi, L. Liu, G. Bertrand, *Org. Chem. Front.* **2014**, *1*, 351-354.
- [27] D. C. Georgiou, B. D. Stringer, C. F. Hogan, P. J. Barnard, D. J. D. Wilson, N. Holzmann, G. Frenking, J. L. Dutton, *Chem. Eur. J.* **2015**, *21*, 3377-3386.
- [28] D. C. Georgiou, I. Mahmood, M. A. Haghghatbin, C. F. Hogan, J. L. Dutton, *Pure Appl. Chem.* **2017**, 791-800.
- [29] D. Wu., Y. Li, R. Ganguly, R. Kinjo, *Chem. Commun.* **2014**, *50*, 12378-12381.
- [30] I. Nakanishi, S. Itoh, *Chem. Commun.* **1997**, 1927-1928.
- [31] I. Nakanishi, S. Itoh, S. Fukuzumi, *Chem. Eur. J.* **1999**, *5*, 2810-2818.
- [32] J. K. Mahoney, D. Martin, C. E. Moore, A. L. Rheingold, G. Bertrand, *J. Am. Chem. Soc.* **2013**, *135*, 18766-18769.
- [33] J. K. Mahoney, R. Jazzar, G. Royal, D. Martin, G. Bertrand, *Chem. Eur. J.* **2017**. DOI: 10.1002/chem.201700144
- [34] C. L. Deardorff, R. E. Sikma, C. P. Rhodes, T. W. Hudnall, *Chem. Commun.* **2016**, *52*, 9024-9027.
- [35] M. M. D. Roy, E. Rivard, *Acc. Chem. Res.* **2017**, *50*, 2017-2025.
- [36] K. Powers, C. Hering-Junghans, R. McDonald, M. J. Ferguson, E. Rivard, *Polyhedron*, **2016**, *108*, 8-14.
- [37] C. Poidevin, J. Malrieu, G. Trinquier, C. Lepetit, F. Allouti, M. E. Alikhani, R. Chauvin, *Chem. Eur. J.* **2016**, *22*, 5295-5308.
- [38] M. Asay, B. Donnadiéu, W.W. Schoeller, G. Bertrand, *Angew. Chem. Int. Ed.* **2009**, *48*, 4796-4799; *Angew. Chem.* **2009**, *121*, 4890-4893.
- [39] J. P. Perdew, K. Burke, M. Ernzerhof, *Phys. Rev. Lett.* **1996**, *77*, 3865-3868.
- [40] J. P. Perdew, M. Ernzerhof, K. Burke, *J. Chem. Phys.* **1996**, *105*, 9982-9985.
- [41] J. P. Perdew, K. Burke, M. Ernzerhof, *Phys. Rev. Lett.* **1997**, *78*, 1396.
- [42] C. Adamo, V. Barone, *J. Chem. Phys.* **1999**, *110*, 6158-6170.
- [43] A. Schäfer, C. Huber, R. Ahlrichs, *J. Chem. Phys.* **1994**, *100*, 5829-5835.
- [44] F. Weigend, R. Ahlrichs, *Phys. Chem. Chem. Phys.* **2005**, *7*, 3297-3305.
- [45] R. G. Compton, C. E. Banks, *Understanding Voltammetry*, Imperial College Press, London, **2011**, p. 429.
- [46] We prepared the analogous PPh<sub>3</sub> derivatives, [Ph<sub>3</sub>P-CC-Ph][Br] and [Ph<sub>3</sub>P-CC-C<sub>6</sub>H<sub>4</sub>-CC-PPh<sub>3</sub>][Br]<sub>2</sub>, and noted that for each compound the reduction process was non-reversible by cyclic voltammetry and chemical reduction only gave back trace amounts of PPh<sub>3</sub> as observed by <sup>31</sup>P NMR spectroscopy. Chemistry involving these and related ethynyl phosphonium salts has been reported: A. J. Veinot, A. D. K. Todd, J. D. Masuda, *Can. J. Chem.* **2017**, DOI:10.1139/cjc-2017-0482.
- [47] N.G. Connelly, W. E. Geiger, *Chem. Rev.* **1996**, *96*, 877-910.
- [48] J. A. Januszewski, D. Wendinger, C. D. Methfessel, F. Hampel, R. R. Tykwinski, *Angew. Chem. Int. Ed.* **2013**, *52*, 1817-1821; *Angew. Chem.* **2013**, *125*, 1862-1867.
- [49] Bond Length Alteration value for [3]cumulenes is calculated by the following equation: BLA = [bond length of C<sub>1</sub>=C<sub>2</sub> + bond length of C<sub>3</sub>=C<sub>4</sub>]/2 - [bond length of C<sub>2</sub>=C<sub>3</sub>] where R<sub>2</sub>C<sub>1</sub>=C<sub>2</sub>=C<sub>3</sub>=C<sub>4</sub>R<sub>2</sub>.
- [50] This phenyl substituted [3]cumulene system was reported in 1959 to be not isolable (W. Ried, G. Dankert, *Chem. Ber.*, **1959**, *92*, 1223-1236) and recent calculations show that it is more stable as an open shell singlet biradical.<sup>[40]</sup>
- [51] M. M. Hansmann, M. Melaimi, G. Bertrand, *J. Am. Chem. Soc.* **2017**. DOI:10.1021/jacs.7b09622

## COMMUNICATION

## Entry for the Table of Contents

## COMMUNICATION

Two electron reduction of an *N*-heterocyclic carbene derived bis-imidazolidinium ethynyl dication gives an extended bis-1,4-([3]cumulene)-*p*-carbo-quinoid with no change in the overall distance between the NHC moieties.



Brian M. Barry, R. Graeme Soper, Juha Hurmalainen, Akseli Mansikkamäki, Katherine N. Robertson, William L. McClennan, Alex J. Veinot, Tracey L. Roemmele, Ulrike Werner-Zwanziger, Rene T. Boéré\*, Heikki M. Tuononen\*, Jason A. C. Clyburne\*, Jason D. Masuda\*

Page No. – Page No.

**Mono- and Bis-Imidazolidinium Ethynyl Cations and the Reduction of the Latter to give an Extended Bis-1,4-([3]Cumulene)-*p*-Carbo-Quinoid System**

Supporting Information

**Mono- and Bis(imidazolidinium ethynyl) Cations and Reduction of the Latter To Give an Extended Bis-1,4-([3]Cumulene)-*p*-carboquinoid System\*\***

*Brian M. Barry, R. Graeme Soper, Juha Hurmalainen, Akseli Mansikkamäki, Katherine N. Robertson, William L. McClennan, Alex J. Veinot, Tracey L. Roemmele, Ulrike Werner-Zwanziger, René T. Boéré,\* Heikki M. Tuononen,\* Jason A. C. Clyburne,\* and Jason D. Masuda\**

anie\_201711031\_sm\_miscellaneous\_information.pdf



## Table of Contents

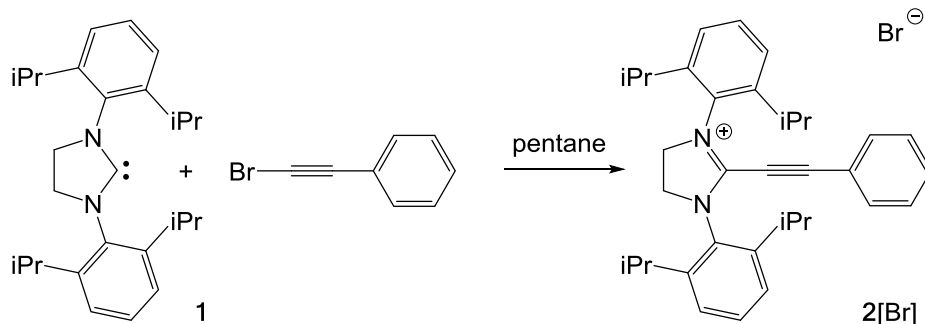
General Synthetic Procedures	S2
Synthesis of Compound <b>2</b>	S3
Synthesis of Compounds <b>2</b> [PF <sub>6</sub> ], <i>para</i> -F- <b>2</b> [PF <sub>6</sub> ], and <i>para</i> -Ph- <b>2</b> [Br].	S5
Synthesis of Compound <b>3</b> [Br]	S6
Inferior Synthesis of Compound <b>3</b> [Br] Contaminated with Compound <b>4</b> [Br]	S8
Synthesis of Compound <b>5</b>	S9
Solid State <sup>13</sup> C NMR Spectroscopy on Compound <b>5</b>	S10
Alternating Current Magnetic Susceptibility Studies, Experimental Conditions and Results on Compound <b>5</b>	S13
Computational Details	S14
Cyclic Voltammetry	S16
X-ray Crystallography	S17
References	S23

## General Synthetic Procedures

All reactions were performed in dry, O<sub>2</sub>-free conditions under an atmosphere of N<sub>2</sub> within an mBraun Labmaster SP inert atmosphere drybox or using standard Schlenk techniques. All reagents were purchased from Sigma-Aldrich and used as received, unless otherwise noted. Alumina and molecular sieves were pre-dried in a 150°C oven before being dried at 250-300°C *in vacuo*. Solvents were purified using an Innovative Technology solvent purification system or purchased as 'anhydrous' from Sigma-Aldrich. Solvents were then dried using KH and subsequently filtered through dry alumina and stored over previously dried 4Å molecular sieves. Glassware was dried at 150°C overnight prior to experimentation. Solution NMR spectra were recorded on a Bruker Avance 300MHz spectrometer. Trace amounts of non-deuterated solvent were used as internal references for <sup>1</sup>H NMR spectra and were referenced relative to tetramethylsilane. The deuterated solvent was used as an internal reference for <sup>13</sup>C{<sup>1</sup>H} NMR spectra and referenced relative to tetramethylsilane. Coupling constants are reported as absolute values. Melting points were recorded on an Electrothermal MEL-Temp 3.0 using glass capillaries sealed under inert conditions and are uncorrected. Ultraviolet-visible (UV-VIS) spectroscopy was performed using a Varian Cary 50 Conc Spectrophotometer. Elemental analysis was performed by the Centre for Environmental Analysis and Remediation (CEAR) facility at Saint Mary's University using a Perkin Elmer 2400 II series Elemental Analyser or by Canadian Microanalytics. SiPr<sup>[1]</sup>, phenyl ethynylbromide<sup>[2]</sup> and 1,4-bis(bromoethynyl)benzene<sup>[2]</sup> were prepared via literature procedures. 4-F-phenyl ethynyl bromide and 4-Ph-phenyl ethynyl bromide were prepared following literature procedures.<sup>[3]</sup> Phenyl ethynylbromide was purified by vacuum distillation and stored at -35°C prior to use.

\*\*\*\*Warning – Although we did not experience any problems, haloalkynes (or their impurities) are known to be explosive. Due diligence must be observed when purifying these materials (e.g. blast shields)\*\*\*\*

## Synthesis of Compound 2[Br]



In a 100-mL Schlenk flask, a pale yellow coloured solution of bromoethynylbenzene (0.281 g, 1.55 mmol, 1.00 eq.) dissolved in 10 mL of pentane was stirred with a PTFE-coated magnetic stir bar. In a separate 20-mL scintillation vial, 0.606 g of colourless SiPr carbene **1** were dissolved in 20 mL of pentane, producing a colorless mixture. The SiPr carbene **1** was not very soluble in pentane, so a PTFE-coated magnetic stir bar was added and the mixture was stirred for 5 minutes before allowing the contents to settle. The colourless supernatant was removed using a pipette and added dropwise to the solution of bromoethynylbenzene, producing a colorless precipitate within minutes. The yellow color also intensified during the addition. This process was repeated once more to dissolve the remaining carbene, requiring a total volume of 40 mL of pentane. The yellow colored reaction mixture was left to stir for 3 h before allowing the contents of the flask to settle and decanting the orange colored supernatant. The pale yellow coloured precipitate was washed twice with 5 mL of pentane, and dried *in vacuo* to yield 0.246 g of the desired compound as a beige colored powder. Additional product was isolated from the combined filtrates as a faintly beige colored powder following a similar work-up procedure, after which was washed once with ca. 10 mL of hot (nearly boiling) heptane and dried *in vacuo* yielding a colorless powder **2[Br]**.

Yield: 0.508 g (57 %); m.p. 244-245 °C; HRMS (ESI): 491.3421; Elemental Analysis calculated for C<sub>35</sub>H<sub>43</sub>BrN<sub>2</sub>: C 73.54, H 7.58, N 4.90 %; Found: C 73.56, H 7.21, N 5.01 %. IR (Nujol mull): 2223 (C≡C) cm<sup>-1</sup>. UV-Vis: 376 nm (ε = 386 Lmol<sup>-1</sup>cm<sup>-1</sup>).

<sup>1</sup>H-NMR (300MHz, CDCl<sub>3</sub>): δ 7.66 (tt, <sup>3</sup>J<sub>HH</sub> = 7.6 Hz, <sup>4</sup>J<sub>HH</sub> = 1.3 Hz, 1H, *p*-PhH), 7.55 (t, <sup>3</sup>J<sub>HH</sub> = 7.8 Hz, 2H, *p*-DippH), 7.34 (d, <sup>3</sup>J<sub>HH</sub> = 7.8 Hz, 4H, *m*-DippH), 7.26 (m, <sup>3</sup>J<sub>HH</sub> = 8.0 Hz, <sup>3</sup>J<sub>HH</sub> = 7.7 Hz, 2H, *m*-PhH), 6.82 (dd, <sup>3</sup>J<sub>HH</sub> = 8.3 Hz, <sup>4</sup>J<sub>HH</sub> = 1.3 Hz, 2H, *o*-PhH), 4.96 (s, 4H, SiPr-CH<sub>2</sub>), 3.06 (sept, <sup>3</sup>J<sub>HH</sub> = 6.8 Hz, 4H, <sup>i</sup>Pr-CH), 1.42 (d, <sup>3</sup>J<sub>HH</sub> = 6.8 Hz, 12H, <sup>i</sup>Pr-CH<sub>3</sub>), 1.25 ppm (d, <sup>3</sup>J<sub>HH</sub> = 6.8 Hz, 12H, <sup>i</sup>Pr-CH<sub>3</sub>). <sup>13</sup>C {<sup>1</sup>H}-NMR (300 MHz, CDCl<sub>3</sub>): δ 152.2, 146.7, 133.3 (s, *p*-(C<sub>6</sub>H<sub>5</sub>)), 133.0 (s, *o*-(C<sub>6</sub>H<sub>5</sub>)), 131.6 (s, *p*-DippC), 129.9 (s), 129.3 (s, *m*-(C<sub>6</sub>H<sub>5</sub>)), 125.1 (s, *m*-DippC), 116.4 (s), 110.4 (s, SiPr-C≡C-Ph), 72.4 (s, SiPr-C≡C-Ph), 55.0 (s, SiPr-CH<sub>2</sub>), 29.5 (s, <sup>i</sup>Pr-CH), 24.8 (s, <sup>i</sup>Pr-CH<sub>3</sub>), 24.4 ppm (s, <sup>i</sup>Pr-CH<sub>3</sub>).

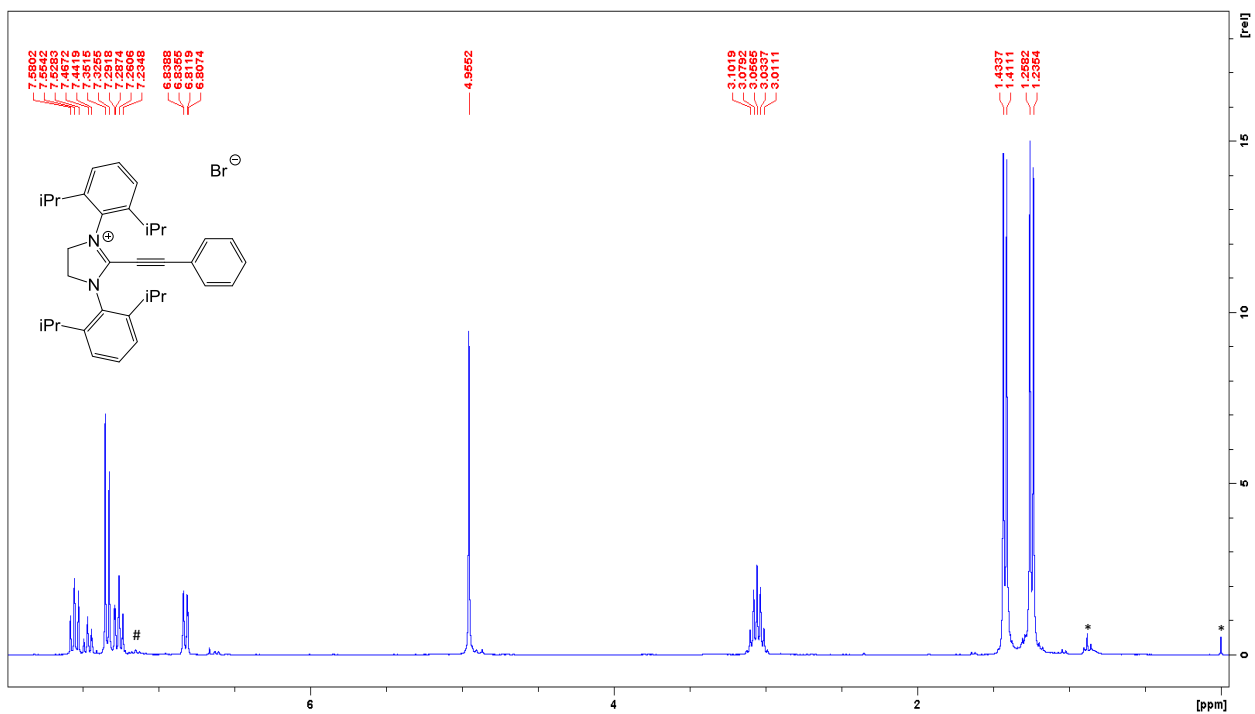


Figure S1:  $^1\text{H}$  NMR spectrum of Compound 2[Br] in  $\text{CDCl}_3$ . \* denotes impurity. # denotes residual  $\text{CHCl}_3$

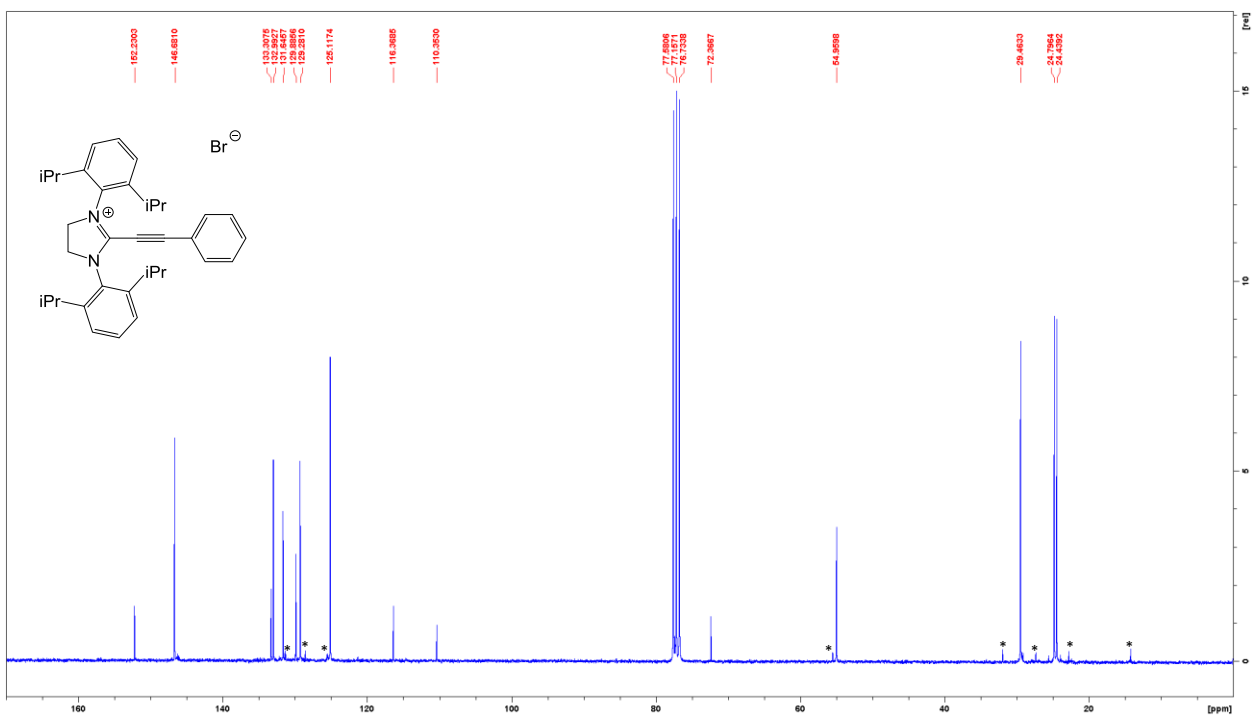
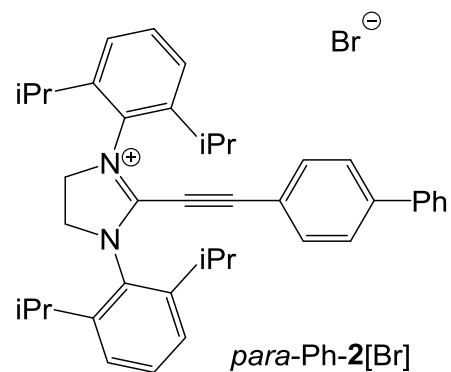
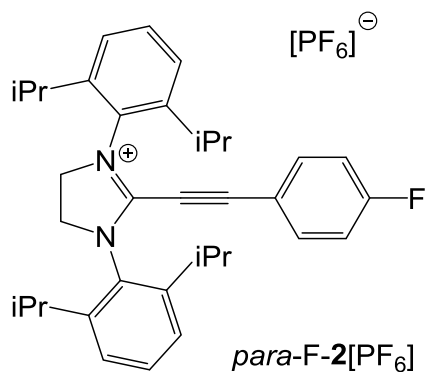
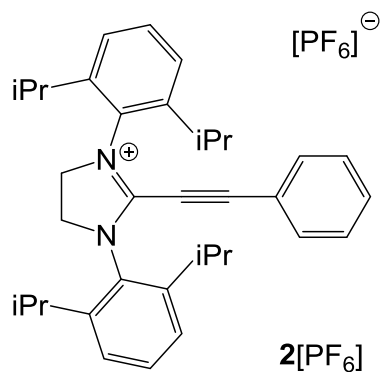


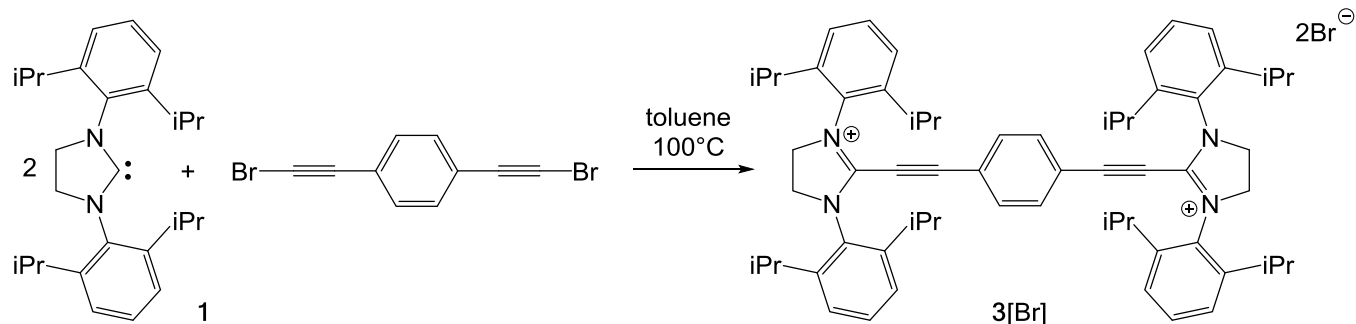
Figure S2:  $^{13}\text{C}$  NMR spectrum of compound 2[Br] in  $\text{CDCl}_3$ . \* denotes impurity

## Synthesis of Compounds **2**[PF<sub>6</sub>], *para*-F-**2**[PF<sub>6</sub>], and *para*-Ph-**2**[Br]

These compounds were prepared in a manner similar to compound **2**[Br] and only characterized by single crystal X-ray diffraction. Crystals were grown from dichloromethane/pentane mixtures. Compounds **2**[PF<sub>6</sub>] and *para*-F-**2**[PF<sub>6</sub>] were obtained after metathesis with KPF<sub>6</sub>.



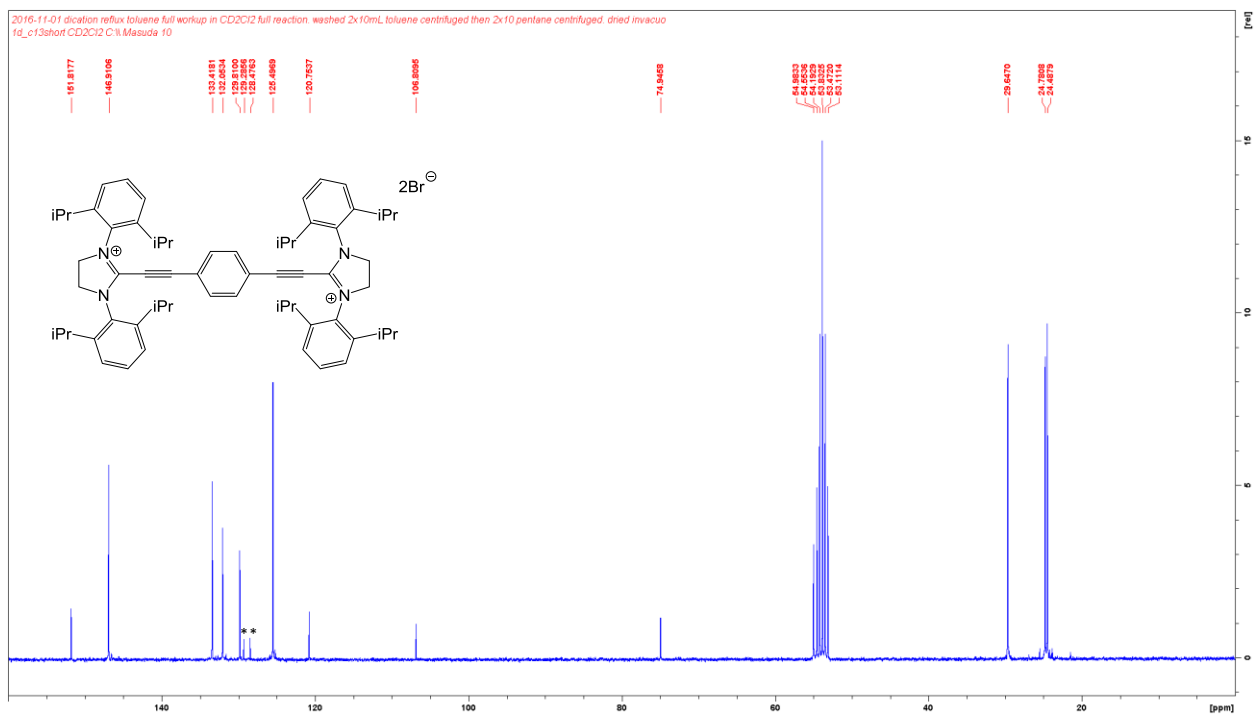
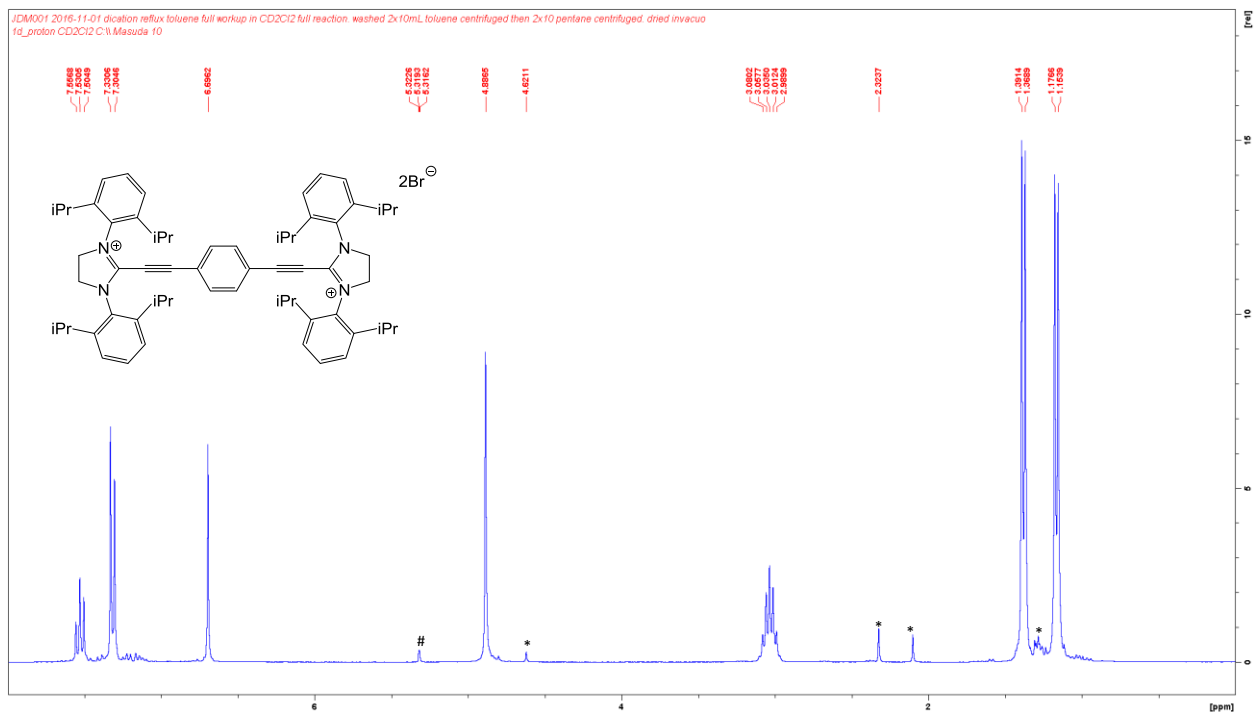
## Synthesis of Compound 3[Br]



To a 50 mL reaction vessel containing a PTFE-coated stir bar a solution of the SiPr carbene **1** (1.408 g, 3.60 mmol) in *ca.* 20 ml of toluene was added to a solution of 1,4-*bis*(bromoethynyl)benzene (0.512 g, 1.80 mmol) in *ca.* 10 ml of toluene. The resulting yellow/brown colored solution was heated with stirring at 100°C overnight. The resulting tan colored powder was separated from the toluene by centrifugation. The powder was washed 2x10 mL toluene, followed by 2x10 mL pentane, each time treated by centrifugation to allow for easy separation. Residual solvent was removed *in vacuo* to give compound **3[Br]** as a light tan colored powder.

Yield = 1.703 g (88.6%); m.p. 257.4-257.9°C (darkens/decomp); Elemental Analysis calculated for C<sub>64</sub>H<sub>80</sub>Br<sub>2</sub>N<sub>4</sub>: C 72.17, H 7.57, N 5.26, %; Found: C 71.03, H 7.60, N 5.13. IR (Nujol mull): 2227 (C≡C) cm<sup>-1</sup>. UV-Vis: 314 nm (ε = 4186 Lmol<sup>-1</sup>cm<sup>-1</sup>).

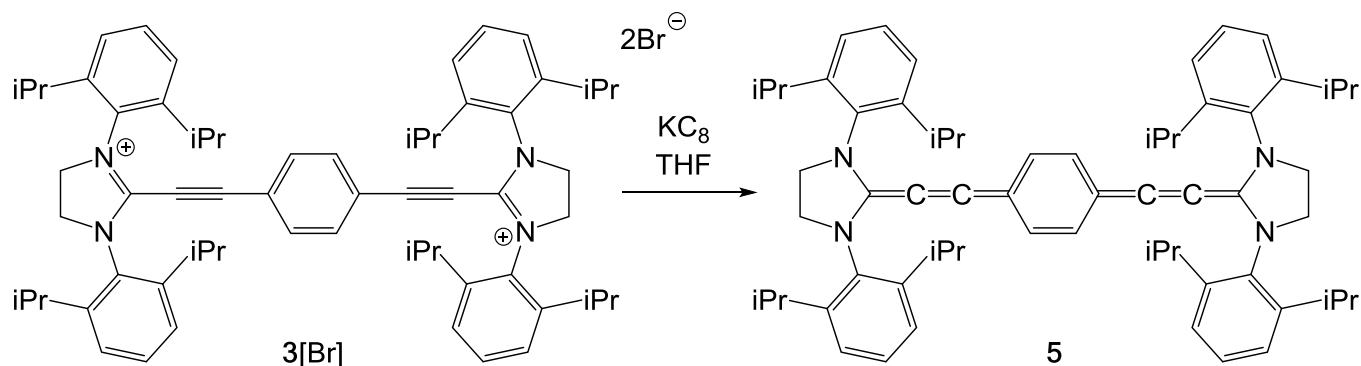
<sup>1</sup>H NMR (300MHz, CD<sub>2</sub>Cl<sub>2</sub>): δ 1.16 (d, <sup>3</sup>J<sub>H-H</sub> = 6.9Hz, 24H, (CH<sub>3</sub>)<sub>2</sub>CH), 1.38 (d, <sup>3</sup>J<sub>H-H</sub> = 6.9Hz, 24H, (CH<sub>3</sub>)<sub>2</sub>CH), 3.04 (sept, <sup>3</sup>J<sub>H-H</sub> = 6.9 Hz, 8H, (CH<sub>3</sub>)<sub>2</sub>CH), 4.89 (s, 8H, CH<sub>2</sub>), 6.70 (s, 4H, C<sub>6</sub>H<sub>4</sub>), and 7.32 (d, <sup>3</sup>J<sub>H-H</sub> = 7.7Hz, 8H, *m*-Dipp), 7.32 (t, <sup>3</sup>J<sub>H-H</sub> = 7.7Hz, 4H, *p*-Dipp) ppm. <sup>13</sup>C NMR (75MHz, CD<sub>2</sub>Cl<sub>2</sub>): δ 24.49, 24.78, 29.65, 54.98, 74.95, 109.81, , 120.75, 125.50, 129.81, 132.05, 133.42, 146.91, 151.82 ppm.







## Synthesis of Compound 5



A suspension of **3[Br]** (0.400 g, 0.375 mmol) in *ca.* 5 ml of THF was added to a suspension of  $\text{KC}_8$  (0.1522 g, 1.13 mmol) in *ca.* 10 ml of THF, resulting in a black colored solution. This mixture was stirred at room temperature overnight, and the solvent was removed *in vacuo* resulting in a black solid. The residual solid was extracted with pentane (3x10 ml) then filtered through a bed of diatomaceous earth resulting in an intensely colored blue-violet solution. The solvent was removed *in vacuo* yielding compound **5** as a dark violet crystalline material.

Yield = 0.1129 g (33%); m.p. 125-129 °C; IR (nujol mull): 2082(C=C=C)  $\text{cm}^{-1}$ . Elemental Analysis  $\text{C}_{64}\text{H}_{80}\text{N}_4$ : C 84.91, H 8.91, N 6.19.; found: C 84.98, H 8.84 N 5.60. UV-Vis: 278 nm ( $\epsilon = 10441 \text{ Lmol}^{-1}\text{cm}^{-1}$ ), 595 nm ( $\epsilon = 23970 \text{ Lmol}^{-1}\text{cm}^{-1}$ ), 628 nm ( $\epsilon = 16103 \text{ Lmol}^{-1}\text{cm}^{-1}$ ).

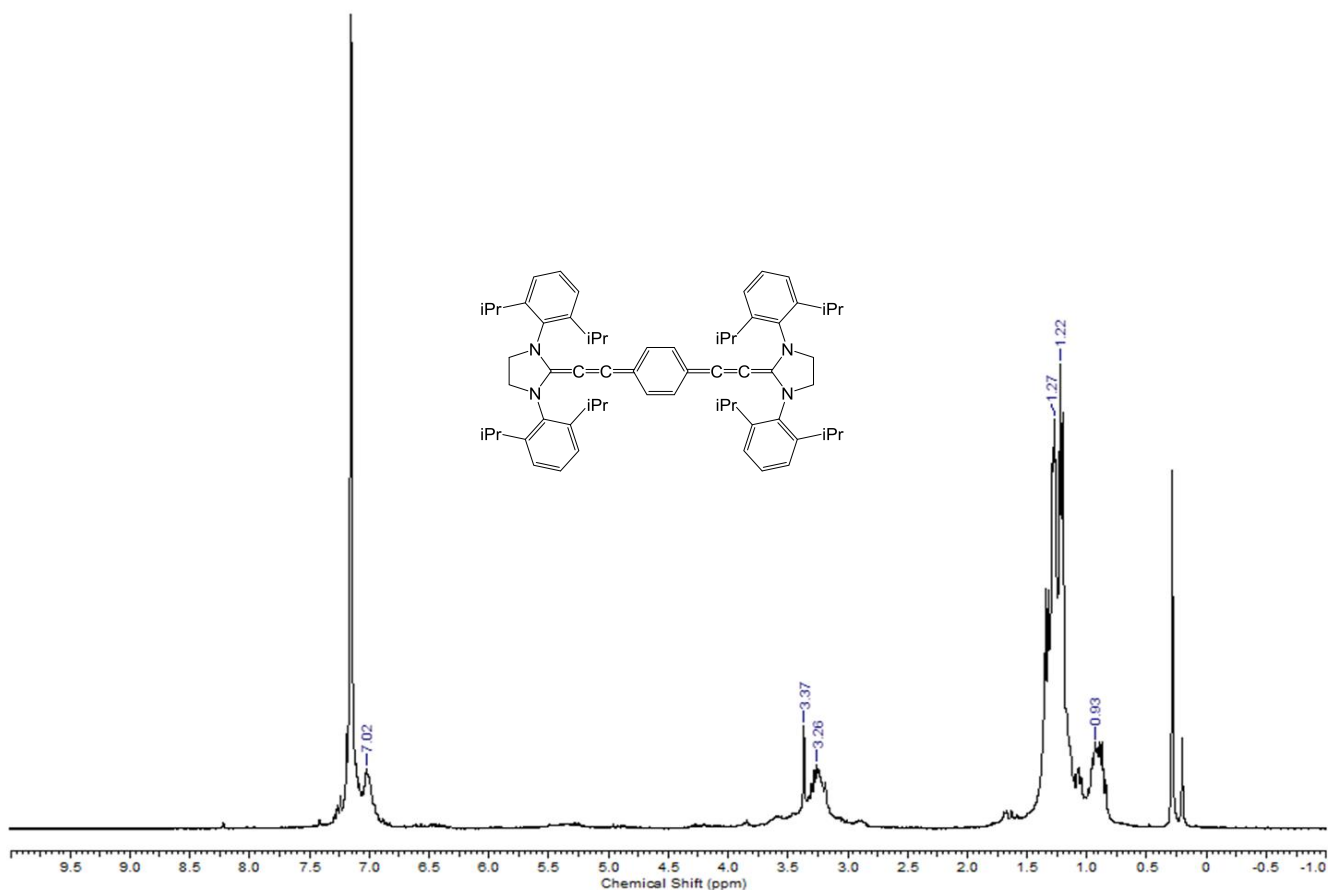


Figure S6:  $^1\text{H}$  NMR spectrum of compound **5** in  $\text{C}_6\text{D}_6$ .

## Solid State $^{13}\text{C}$ NMR Spectroscopy on Compound 5

The  $^{13}\text{C}$  cross-polarization (CP)/ Magic Angle Spinning (MAS) experiments with TPPM proton decoupling were carried out on a Bruker Avance NMR spectrometer with a 9.4T magnet (400.24 MHz proton Larmor frequency, 100.64 MHz  $^{13}\text{C}$  Larmor frequency). Using a probe head for rotors of 4 mm diameter two  $^{13}\text{C}$  CP/MAS NMR spectra were acquired at 5.0 and 7.0 kHz rotation frequencies, accumulating up to 552 scans with cross-polarization times of 2.6 ms. The repetition delays (4.9 s) were chosen to be -ve times the proton spin lattice relaxation time,  $T_1$ , measured by inversion-recovery sequence. The  $^{13}\text{C}$  CP/MAS powers were optimized on glycine, whose carbonyl resonance also served as external, secondary chemical shift standard at 176.06 ppm.

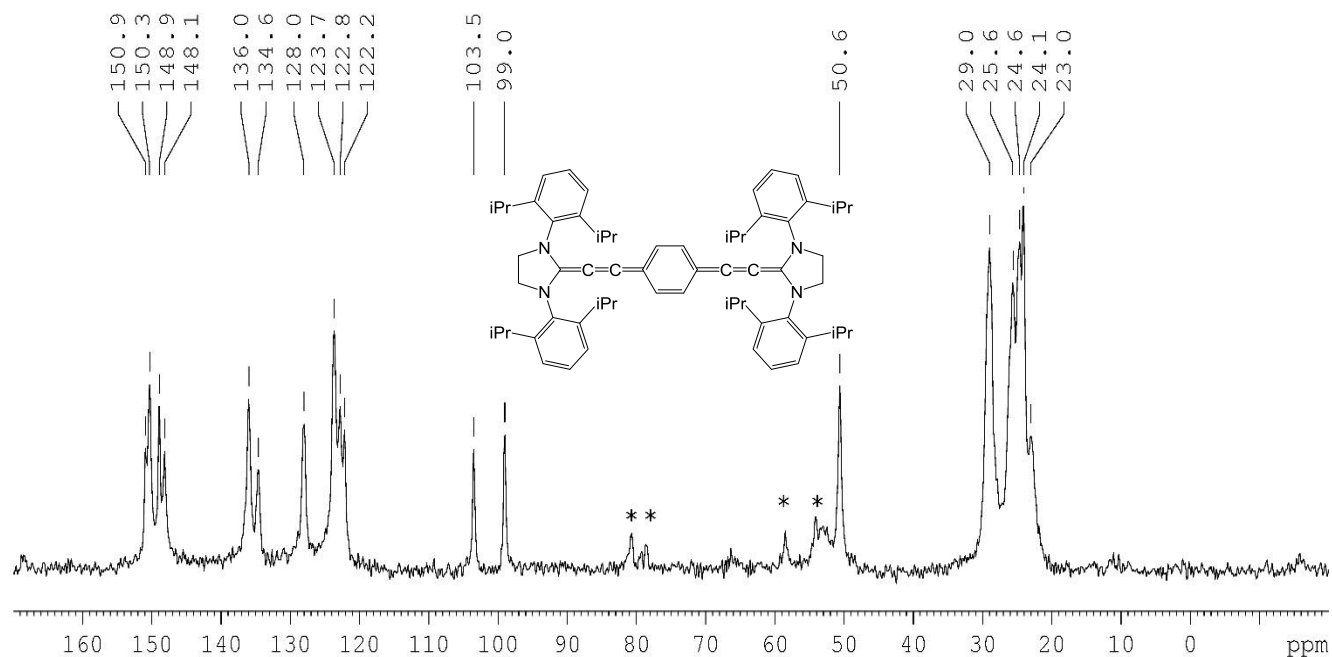


Figure S7:  $^{13}\text{C}$  SSNMR spectrum of compound 5. Only the isotropic shifts are specified, spinning side bands are labeled with \*.

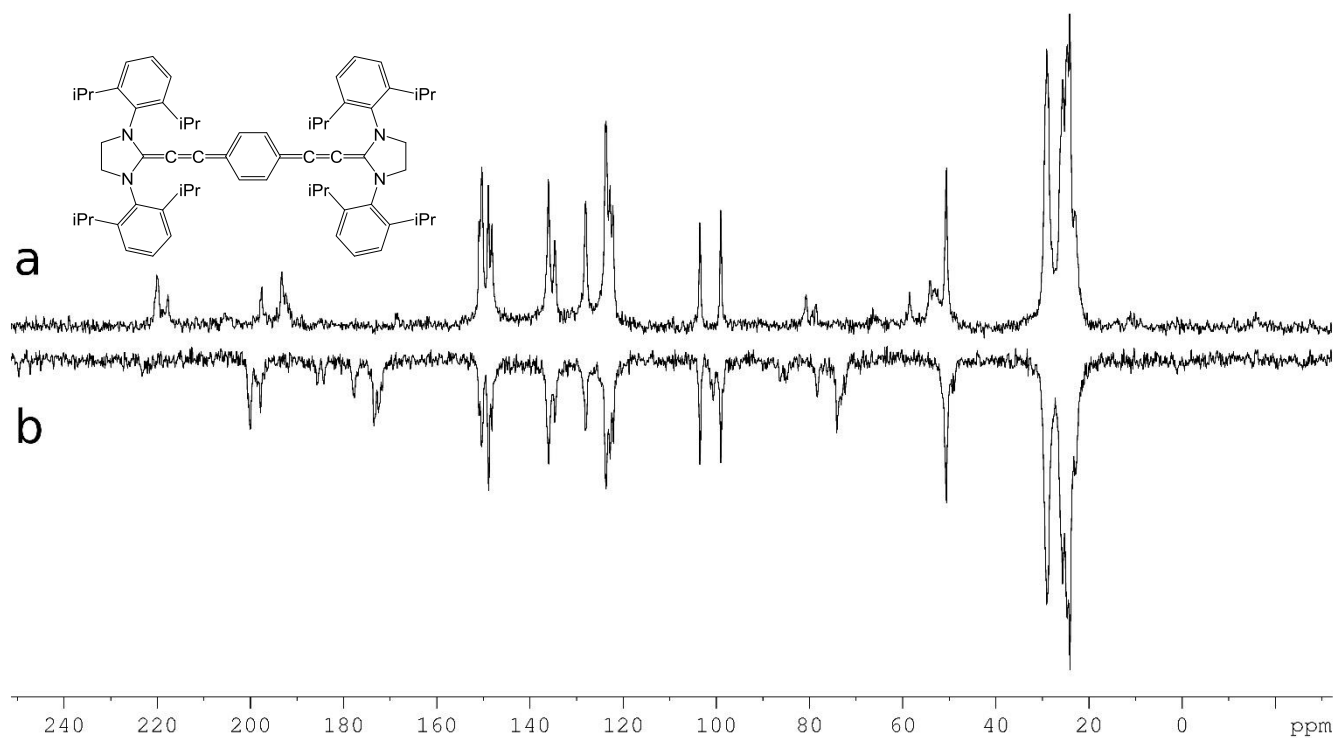


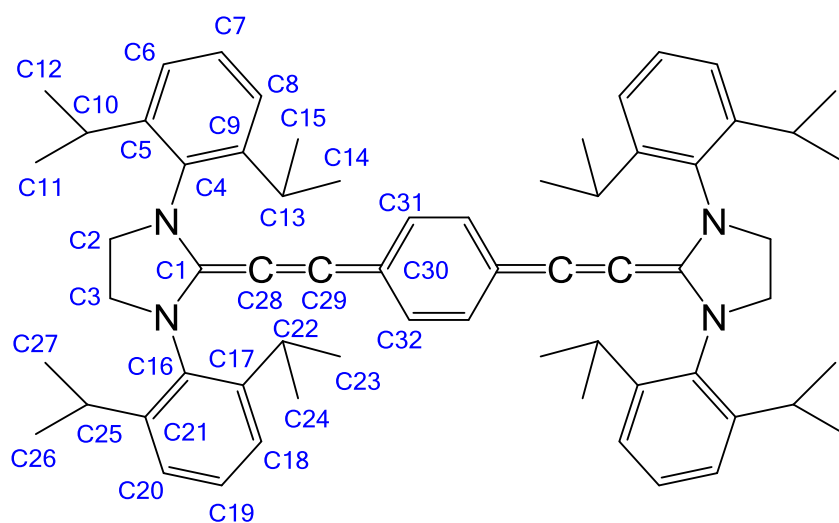
Figure S8:  $^{13}\text{C}$  SSNMR spectra of compound **5** at 7.0 kHz MAS (a) and 5.0 kHz MAS (b). Peaks that shift with spinning frequency are due to spinning sidebands.

Table S1: Tabulated Values of Spinning Side Band Peaks (SSB) of top spectrum (a) in Figure S8

SSB (ppm)
220.0
217.7
197.5
193.3
80.7
66.7
58.5
54.1
53.0

Table S2:  $^{13}\text{C}$  SSNMR Assignments (ppm) of Compound 5

	Experimental	Calculated		
		Optimized $C_i$	Idealized $D_{2d}$	X-ray $C_i$
C1	134.6	140	144	142
C2/3	50.6	52	52	41
C4/16	136.0	141	141	144
C5/9/17/21	148.9/148.1	157	156	158
C6/8/18/20	122.8/122.2	130	129	125
C7/19	128.0	134	133	129
C10/13/22/25	29.0	31	32	24
C11/12/14/15/23/24/26/27	25.6/24.6/24.1/23.0	26	27	3
C28	103.5	113	106	112
C29	150.9/150.3	163	162	163
C30	99.0	103	101	102
C31/32	123.7	127	126	122



## Alternating Current Magnetic Susceptibility Studies, Experimental Conditions and Results on Compound 5

Alternating Current Magnetic Susceptibilities (ACMS) experiments were carried out on a Physical Properties Measurement System (PPMS) by Quantum Design with a working temperature range of 2 - 350 K, equipped with a  $\pm 9$ T magnet. The ACMS experiment (DC magnetization in this case) was calibrated with palladium as a reference. A measurement was taken on the PPMS at constant field and temperature and using the known theoretical magnetic moment for the Pd which varies according to specific magnetic field/temperature. The difference of these two, calculated and measured, was then in turn calculated. The calibration process was repeated until the difference between measured and theoretical was less than 0.01 %. The sample space was held at a vacuum of  $10^{-5}$  Torr. The sample's magnetization was measured as a function of temperature (from 300 - 3 K) under a constant applied field of 1000 Oersted (Oe). The key result of this experiment is that all the magnetic susceptibility values are negative, consistent with a diamagnetic material.

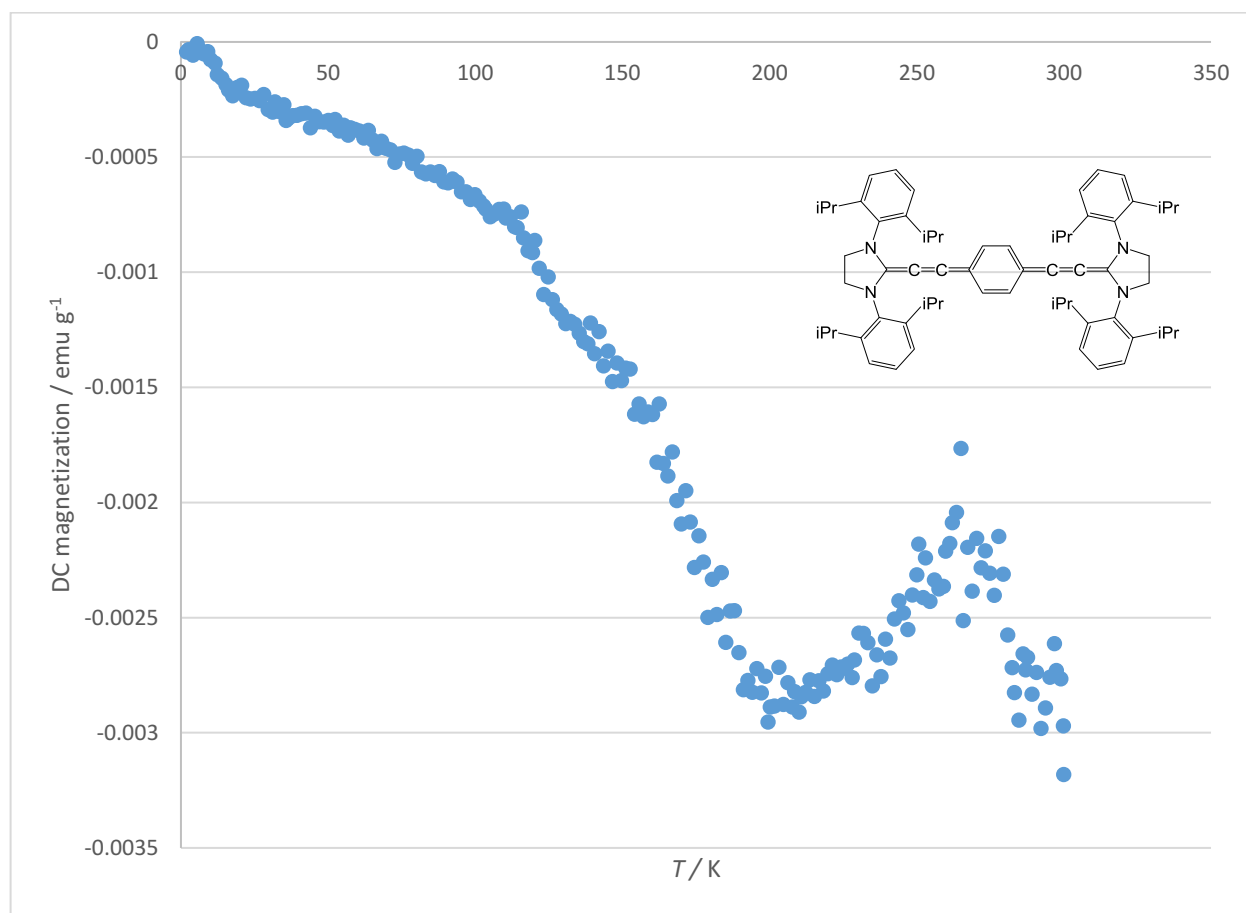


Figure S9: Plot of DC magnetizations ( $\text{emu g}^{-1}$ ) vs. temperature (K) of compound 5.

## Computational Details

All calculations were performed with the Gaussian 09 program.<sup>[4]</sup> Density functional theory (DFT) was used at the PBE1PBE level of theory<sup>[5]</sup> together with Ahlrics' TZVP (geometries and properties) and def2-TZVP (geometries) basis sets.<sup>[6,7]</sup> Chemical shift calculations were performed using the GIAO formalism<sup>[8]</sup> and nucleus independent chemical shift data are reported as NICS(1)<sub>zz</sub> values in which only the magnitude of the tensor perpendicular to the plane of the ring is used.<sup>[9]</sup> Excited state calculations used the time-dependent (TD) approach.<sup>[10]</sup> The effect of solvent (n-pentane) was taken into account *via* IEFPCM solvent model.<sup>[11]</sup>

The gas-phase optimized structure of **2** has  $C_{2v}$  point group with bond lengths and angles that are in excellent agreement with those observed for the cation in the X-ray structure of **2**[Br]. The most notable difference between the calculated and experimental structures is observed for the  $C_{\text{NHC}}\text{-C}\equiv\text{C}$  angle that is linear in the former and bent in the latter. We note that the lowest calculated vibrational mode of **2** is less than  $10\text{ cm}^{-1}$ , which suggests that the structure (in particular, the capping imidazolidine ring and its diisopropylphenyl substituents) can be easily perturbed in the solid state by anion $\cdots$ cation contacts, co-crystallized solvent molecules or other weak interactions. Furthermore, a relaxed geometry scan showed that if the  $C_{\text{NHC}}\text{-C}\equiv\text{C}$  angle in **2** is bent from linear to  $167.3^\circ$  (value in the X-ray crystal structure), the energy increases only *ca.*  $5\text{ kJ mol}^{-1}$ . This demonstrates that the potential for angle bending is very shallow.

Two distinct stationary points were found for the dication **3**: one with  $C_i$  symmetry and another one with  $D_2$  point group. Irrespective of the size of the employed basis set, the  $C_i$  symmetric structure was found to be lower in energy, though only by *ca.*  $1\text{ kJ mol}^{-1}$ . The optimized geometrical parameters are in excellent agreement with those observed for the dication in the X-ray structure of **3**[Br]. The most notable difference between the calculated and experimental structures is observed for the  $C_{\text{NHC}}\text{-C}\equiv\text{C}$  angles that are linear in the former and bent in the latter. Also notable is the conformation of the imidazolidine ring that is planar in the optimized structure but slightly twisted in the X-ray structure. We note that for both  $C_i$  and  $D_2$  symmetric structures, the lowest calculated vibrational modes are less than  $10\text{ cm}^{-1}$ , which suggests that the structure (in particular, the capping imidazolidine rings and their diisopropylphenyl substituents) can be easily perturbed in the solid state by anion $\cdots$ cation contacts, co-crystallized solvent molecules or other weak interactions. Furthermore, a relaxed geometry scan showed that if the  $C_{\text{NHC}}\text{-C}\equiv\text{C}$  angle in **2** is bent from linear to  $163.9^\circ$  (value in the X-ray crystal structure), the energy increases only *ca.*  $10\text{ kJ mol}^{-1}$ . This demonstrates that the potential for angle bending is very shallow.

Two distinct stationary points were found for the cumulene **5**: one with  $C_i$  symmetry and another one with  $C_s$  point group. Irrespective of the size of the employed basis set, the  $C_i$  symmetric structure was found to be lower in energy, though only by *ca.*  $1\text{ kJ mol}^{-1}$ . The optimized geometrical parameters are in excellent agreement with those observed for the cumulene in the X-ray structure of **5**. The most notable difference between the calculated and experimental structures is observed for the  $C_{\text{NHC}}\text{-C}\equiv\text{C}$  angles that are linear in the former and bent in the latter. We note that for both  $C_i$  and  $C_s$  symmetric structures, the lowest calculated vibrational modes are less than  $10\text{ cm}^{-1}$ , which suggests that the structure (in particular, the capping imidazolidine rings and their diisopropylphenyl substituents) can be easily perturbed in the solid state by weak interactions such as dispersion forces. Furthermore, a relaxed geometry scan showed that if the  $C_{\text{NHC}}\text{-C}\equiv\text{C}$  angle in **5** is bent from linear to  $167.0^\circ$  (value in the X-ray crystal structure), the energy increases only *ca.*  $15\text{ kJ mol}^{-1}$ . This demonstrates that the potential for angle bending is very shallow.

One noteworthy observation from the optimized geometries of **3** and **5** is the almost non-existent shortening of the carbon $\cdots$ carbon separation in the phenylethynylimidazolidinium framework upon addition of two electrons. The distance between the two  $C_{\text{NHC}}$  atoms in the dication **3** is  $10.84\text{ \AA}$ , whereas the corresponding distance in the neutral cumulene **5** is  $10.74\text{ \AA}$ . Consequently, there is only  $0.10\text{ \AA}$  (*ca.*  $1\%$ ) difference between the two  $C_{\text{NHC}}\cdots C_{\text{NHC}}$  distances in these two structures. This is also what is observed when comparing the crystal structures of **3**[Br] and **5**.

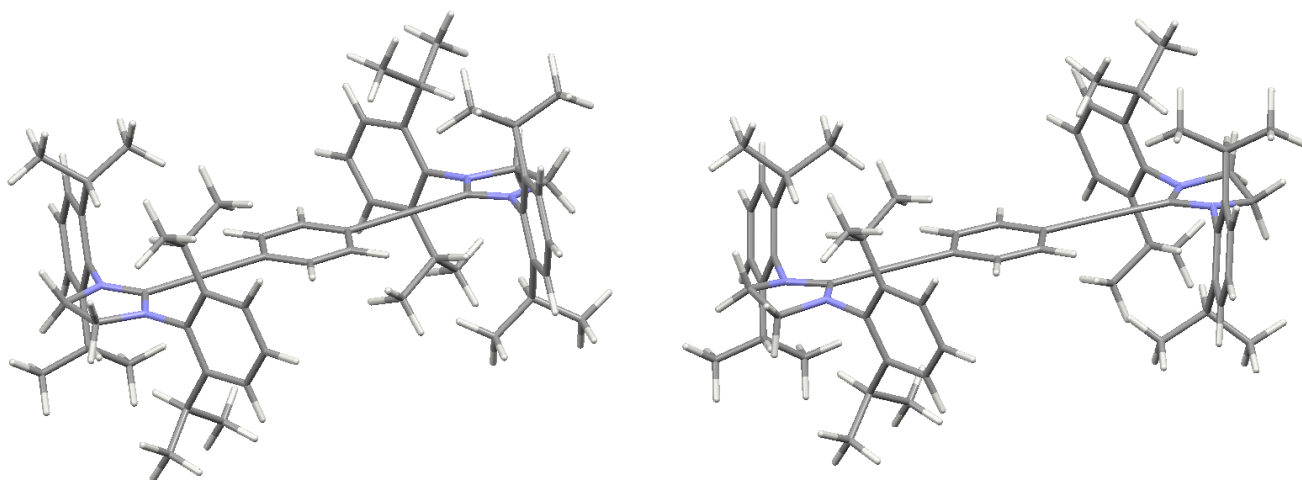


Figure S10: Optimized geometries of dication **3** (left) and cumulene **5** (right).

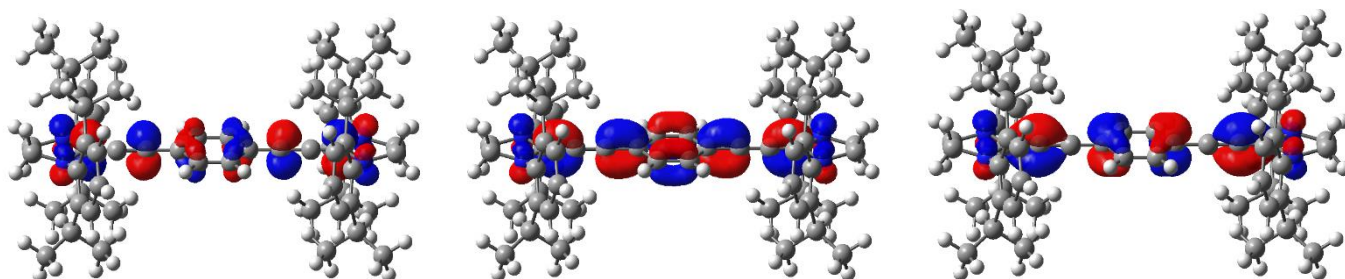


Figure S11: Frontier orbitals of cumulene **5**: LUMO (left), HOMO (middle), and HOMO-1 (right).

## Cyclic Voltammetry

Cyclic voltammetry (CV) and square wave (SW) studies were performed in CH<sub>3</sub>CN or CH<sub>2</sub>Cl<sub>2</sub> solutions inside an inert atmosphere MBraun MB10 Compact Labstar electrochemical glove box at room temperature using both platinum and glassy carbon electrodes and [nBu<sub>4</sub>N][PF<sub>6</sub>] (0.1 M) as the electrolyte. CV and SW measurements were performed with a Princeton Applied Research PARSTAT 2273 potentiostat.

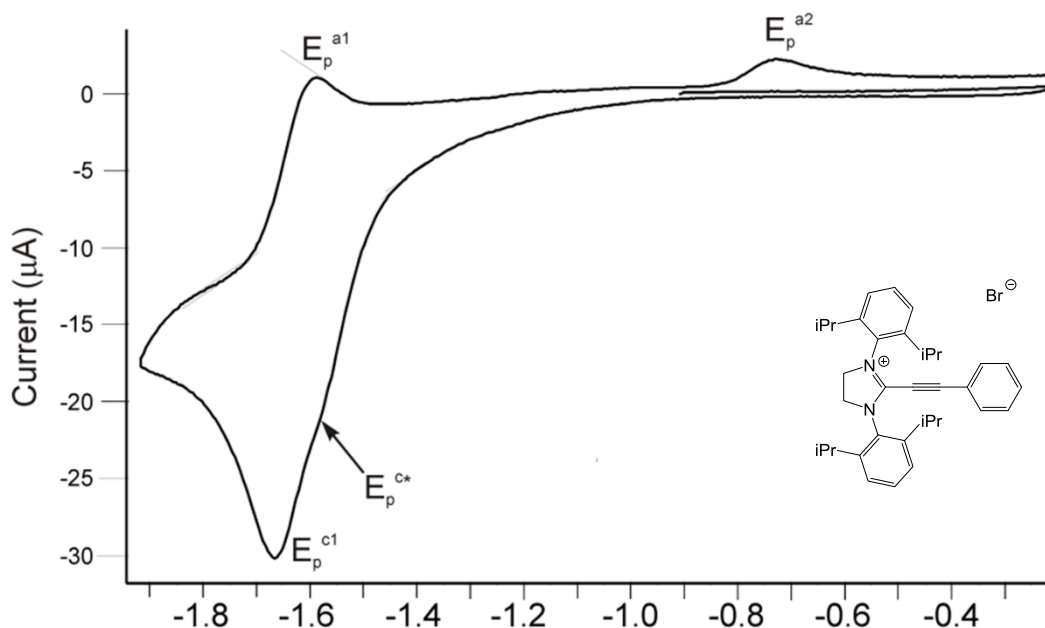


Figure S12: CV of **2**[Br] in CH<sub>3</sub>CN containing 0.1 M [nBu<sub>4</sub>N][PF<sub>6</sub>] at a Pt electrode at room temperature; sweep rate 0.2 V s<sup>-1</sup> with the potential starting at -0.9 V and sweeping in the anodic direction first.

Table S3: CV Data Obtained for **2**[Br] in CH<sub>3</sub>CN<sup>a</sup>

Compound	Electrode	E <sub>p</sub> <sup>c1</sup> (V)	E <sub>p</sub> <sup>a1</sup> (V)	E <sub>m</sub> (V) <sup>b</sup>	E <sub>p</sub> <sup>a2</sup> (V)	E <sub>p</sub> <sup>c2</sup> (V)	E <sub>n</sub> (V) <sup>c</sup>	E <sub>p</sub> <sup>c*</sup> (V)
<b>2</b> [Br]	Pt	-1.67	-1.59	-1.63	-0.73	—	—	-1.57
<b>2</b> [Br]	GC	-1.68	-1.60	-1.64	-0.73	—	—	-1.59

<sup>a</sup> Obtained at room temperature using sweep rate 0.2 V s<sup>-1</sup> and 0.1 M [nBu<sub>4</sub>N][PF<sub>6</sub>].

<sup>b</sup> E<sub>m</sub> = [E<sub>p</sub><sup>a1</sup> + E<sub>p</sub><sup>c1</sup>]/2 ≈ E<sup>o</sup><sub>(1)</sub>.

<sup>c</sup> E<sub>n</sub> = [E<sub>p</sub><sup>a2</sup> + E<sub>p</sub><sup>c2</sup>]/2 ≈ E<sup>o</sup><sub>(2)</sub>.

The reduction of **2**[Br] was found to be a scan-rate dependent process, whereby the anodic peak current increased upon faster scanning ( $\nu = 0.2\text{--}20\text{ V s}^{-1}$ ) ( $E_m = -1.63\text{ V vs Fc}^{0/+}$ ). No processes were observed upon initial scanning in the anodic direction to 0 V. However, upon scanning first in the cathodic direction an induced process was observed at  $E = -0.73\text{ V vs Fc}^{0/+}$  (see Supporting Information). The peak current for this process was small and *decreased* with increasing scan rate (such a peak was not observed in scans greater than 10 V s<sup>-1</sup>). We attribute these observations to two competing processes (*i.e.* an ECE mechanism<sup>[12]</sup>): (1) a one electron reduction to a short-lived neutral radical, which can be oxidized back to the cation at high scan rates, and, (2) at lower scan rates, the radical undergoes a structural reorganization or chemical decomposition which is responsible for the offset oxidation at -0.73V.



## X-ray Crystallography

Measurements were made on a Bruker APEX II CCD equipped diffractometer (30 mA, 50 kV) using monochromated Mo K $\alpha$  radiation ( $\lambda = 0.71073 \text{ \AA}$ ) at 125K.<sup>[13]</sup> A small crystal was attached to the tip of a MicroLoop with paratone-N oil. The initial orientation and unit cell were indexed using a least-squares analysis of a random set of reflections collected from three series of  $0.5^\circ$   $\omega$ -scans, 10 seconds per frame and 12 frames per series, that were well distributed in reciprocal space. For most data collections, a minimum of four  $\omega$ -scan frame series were collected with  $0.5^\circ$  wide scans, and 366 frames per series at varying  $\phi$  angles ( $\phi = 0^\circ, 90^\circ, 180^\circ, 270^\circ$ ). The crystal to detector distance was set to 6 cm and for most structures a complete sphere of data (or more) was collected. Cell refinement and data reduction were performed with the Bruker SAINT<sup>[14]</sup> software, which corrects for beam inhomogeneity, possible crystal decay, Lorentz effects and polarisation effects. A multi-scan absorption correction was applied (SADABS).<sup>[15]</sup> The structures were solved using either Superflip<sup>[16]</sup> and EDMA<sup>[17]</sup> or SHELXT-2014<sup>[18]</sup> and refined using a full-matrix least-squares method on  $F^2$  with SHELXL-2014.<sup>[19]</sup> The non-hydrogen atoms were refined anisotropically. Hydrogen atoms bonded to carbon were included at geometrically idealized positions and were not refined. The isotropic thermal parameters of the hydrogen atoms were fixed at  $1.2U_{\text{eq}}$  of the parent carbon atom ( $1.5U_{\text{eq}}$  was used for methyl hydrogens).

Three molecules of toluene were included in the crystal structure of compound **2**[Br]. One of these was found to be disordered and all of its atoms were split over two positions. The occupancies of the two parts were refined to a 62/38 % ratio. A rigid bond restraint was placed over each part of the disordered molecule and also over the pendant phenyl rings of the cations. The Flack parameter was refined to give a value of 0.037(5), slightly above the expected value of zero, but in agreement with the Hooft parameter (0.038(2)). Crystals of the dication **3**[Br] were found to be solvated with both water and dichloromethane, neither of which were disordered. The hydrogen atoms in the water molecule were refined isotropically, with  $U_{\text{iso}}(\text{H})$  equal to  $1.5U_{\text{eq}}(\text{O})$  and with the O-H bond lengths restrained to reasonable distances. The crystals of compound **4**[BPh<sub>4</sub>] were solvated with dichloromethane. This solvent could have been the source of the chlorine that was incorporated into the cation. The occupancies of the chlorine/bromine atoms in the cation were refined and gave a ratio of 0.448 (Br) to 0.552 (Cl). Two reflections were omitted from the refinement as they were partially obscured by the beam stop. The set obtained in this data collection had a low value for  $\text{sine}(\theta_{\text{max}})/\text{wavelength}$  (0.5699). The large and floppy tetraphenylborate anion, together with the large cation, gave crystals that, despite our best efforts, did not diffract well. Crystals of compound **5** also gave problems during data collection. Only very small crystals could be grown that were highly unstable and difficult to mount without appreciable decomposition. The data finally obtained had a high merging  $R$  value (0.23) for both of these reasons. A better set of data could not be obtained even though numerous attempts were made. The refinement itself was unexceptional though extinction was refined in this case. All of the compounds reported in the Supporting Information gave crystals solvated with dichloromethane. In every case, the C-Cl bond lengths in the disordered part of the molecule were restrained to a distance of  $1.75 \text{ \AA}$ . In compounds **2**[PF<sub>6</sub>] and *para*-F-**2**[PF<sub>6</sub>] only one chlorine atom was disordered and this was modelled using two parts of equal occupancy. In *para*-Ph-**2**[Br] one entire molecule was split over two positions and the occupancy of each part refined to give a ratio of 52/48 %.

Table S4: Crystallographic Details for Compounds **2**[Br], **3**[Br], **4**[BPh<sub>4</sub>], **5**, **2**[PF<sub>6</sub>], *para*-F-**2**[PF<sub>6</sub>], and *para*-Ph-**2**[Br]

Compound	<b>2</b> [Br]	<b>3</b> [Br]	<b>4</b> [BPh <sub>4</sub> ]	<b>5</b>	<b>2</b> [PF <sub>6</sub> ]	<i>p</i> -F- <b>2</b> [PF <sub>6</sub> ]	<i>p</i> -Ph- <b>2</b> [Br]
Chemical formula	2(C <sub>35</sub> H <sub>43</sub> N <sub>2</sub> ) •2(Br) •3(C <sub>7</sub> H <sub>8</sub> )	C <sub>64</sub> H <sub>80</sub> N <sub>4</sub> •2(Br) •4(CH <sub>2</sub> Cl <sub>2</sub> ) •2(H <sub>2</sub> O)	C <sub>37</sub> H <sub>42</sub> Br <sub>0.45</sub> Cl <sub>0.55</sub> N <sub>2</sub> •C <sub>24</sub> H <sub>20</sub> B •(CH <sub>2</sub> Cl <sub>2</sub> )	C <sub>64</sub> H <sub>80</sub> N <sub>4</sub>	C <sub>35</sub> H <sub>43</sub> N <sub>2</sub> •F <sub>6</sub> P •2(CH <sub>2</sub> Cl <sub>2</sub> )	C <sub>35</sub> H <sub>42</sub> FN <sub>2</sub> •F <sub>6</sub> P •2(CH <sub>2</sub> Cl <sub>2</sub> )	C <sub>41</sub> H <sub>47</sub> N <sub>2</sub> •Br •3(CH <sub>2</sub> Cl <sub>2</sub> )
Formula mass	1419.64	1440.87	974.32	905.32	806.53	824.53	902.49
Crystal system	monoclinic	triclinic	monoclinic	monoclinic	monoclinic	monoclinic	triclinic
<i>a</i> /Å	12.2578(2)	11.3197(3)	11.4298(15)	8.723(5)	15.985(2)	15.932(2)	12.1838(13)
<i>b</i> /Å	25.1145(5)	12.2283(3)	22.510(3)	16.706(9)	19.267(2)	19.439(2)	12.9293(13)
<i>c</i> /Å	13.2146(3)	13.9846(4)	21.346(3)	19.115(10)	13.8919(16)	13.9053(14)	15.8456(16)
$\alpha$ /°	90	109.188(2)	90	90	90	90	73.5330(10)
$\beta$ /°	96.1080(10)	94.029(2)	97.230(2)	92.723(6)	111.843(2)	111.180(8)	82.6590(10)
$\gamma$ /°	90	95.233(2)	90	90	90	90	77.0850(10)
Unit cell volume/Å <sup>3</sup>	4045.00(14)	1810.23(9)	5448.6(12)	2782(3)	3971.2(8)	4015.6(8)	2327.6(4)
Temperature/K	125(2)	125(2)	125(2)	125(2)	125(2)	125(2)	125(2)
Space group	<i>P</i> 2 <sub>1</sub>	<i>P</i> 1	<i>P</i> 2 <sub>1</sub> / <i>n</i>	<i>P</i> 2 <sub>1</sub> / <i>c</i>	<i>C</i> 2/ <i>c</i>	<i>C</i> 2/ <i>c</i>	<i>P</i> 1
No. of formula units per unit cell, <i>Z</i>	2	1	4	2	4	4	2
No. of reflections measured	70206	28556	47858	26624	19701	9391	23398
No. of independent reflections	19620	9065	8406	5101	3639	3654	8492
<i>R</i> <sub>int</sub>	0.0596	0.0561	0.1055	0.2309	0.0335	0.0976	0.0419
Final <i>R</i> <sub>1</sub> values ( <i>I</i> > 2σ( <i>I</i> ))	0.0392	0.0600	0.0496	0.0982	0.0343	0.0583	0.0402
Final <i>wR</i> ( <i>F</i> <sup>2</sup> ) values ( <i>I</i> > 2σ( <i>I</i> ))	0.0890	0.1420	0.1056	0.1885	0.0813	0.1046	0.0824
Final <i>R</i> <sub>1</sub> values (all data)	0.0523	0.0999	0.1032	0.2276	0.0474	0.1508	0.0682
Final <i>wR</i> ( <i>F</i> <sup>2</sup> ) values (all data)	0.0932	0.1600	0.1278	0.2422	0.0876	0.1362	0.0919
Goodness of fit on <i>F</i> <sup>2</sup>	0.992	1.042	1.007	1.009	1.055	0.988	1.016
CCDC number	1549498	1549499	1549500	1549501	1549502	154950	1549504

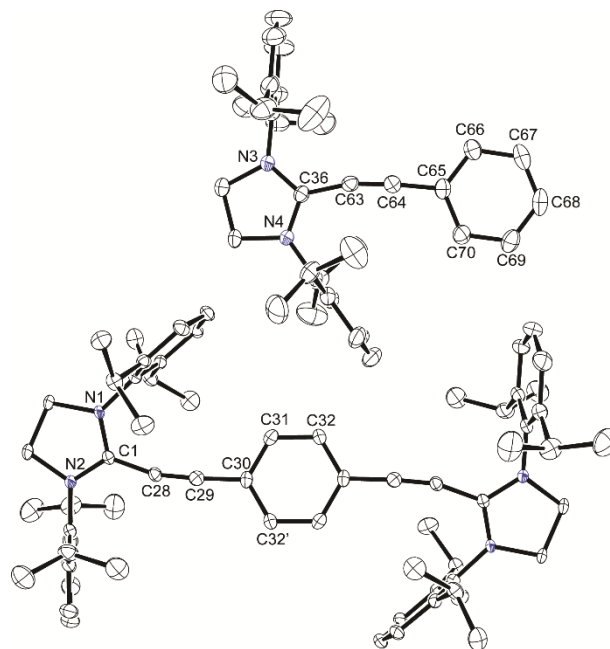


Figure S13. Solid state structure of cation **2** (top, one of two cations in the asymmetric unit) and dication **3** (bottom). Hydrogen atoms, anions, and co-crystallized solvent molecules have been omitted for clarity. Selected bond lengths (Å) and angles (°): **2** N3-C36 1.320(3), N4-C36 1.318(4), C36-C63 1.423(4), C63-C64 1.203(4), C64-C65 1.431(4), C65-C66 1.394(5), C65-C70 1.401(5), C66-C67 1.399(5), C67-C68 1.375(6), C68-C69 1.381(5), C69-C70 1.384(4), N4-C36-N3 113.1(3), N4-C36-C63 121.1(3), N3-C36-C63 125.8(3), C64-C63-C36 167.3(3), C63-C64-C65 175.0(3); **3** N1-C1 1.328(4), N2-C1 1.317(4), 1.478(4), C1-C28 1.417(4), C28-C29 1.197(4), C29-C30 1.430(4), C30-C31 1.399(5), C31-C32 1.386(4), C30-C32' 1.388(4), N2-C1-N1 112.7(3), C29-C28-C1 163.9(3), C28-C29-C30 176.2(3).

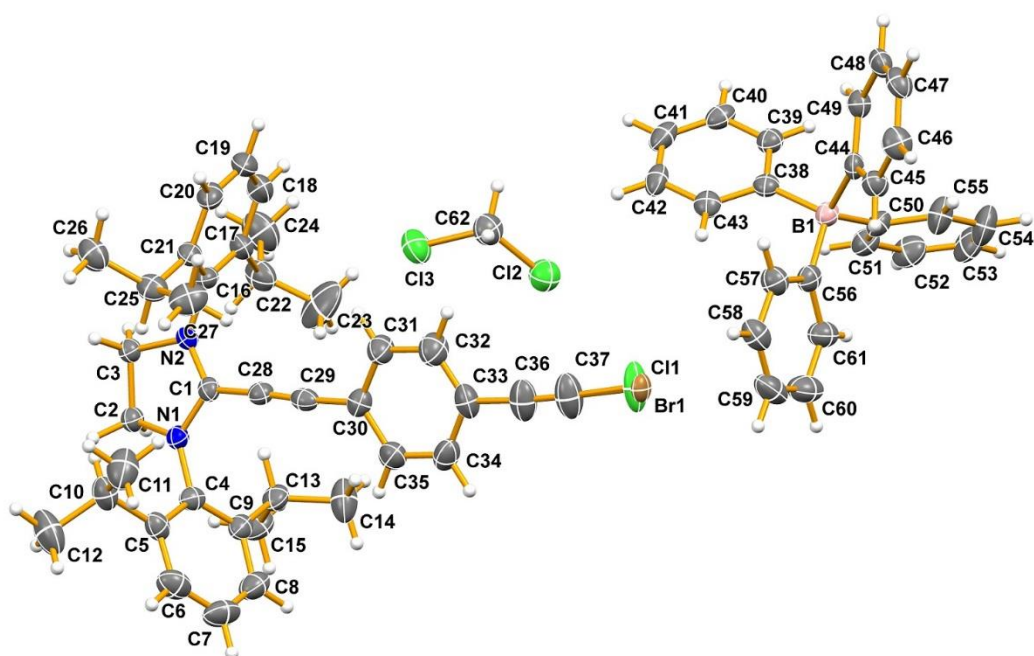


Figure S14: Solid state structure of compound **4**[BPh<sub>4</sub>] with co-crystallized dichloromethane. The ratio of Cl to Br in the cation refined to 55% Cl and 45% Br.

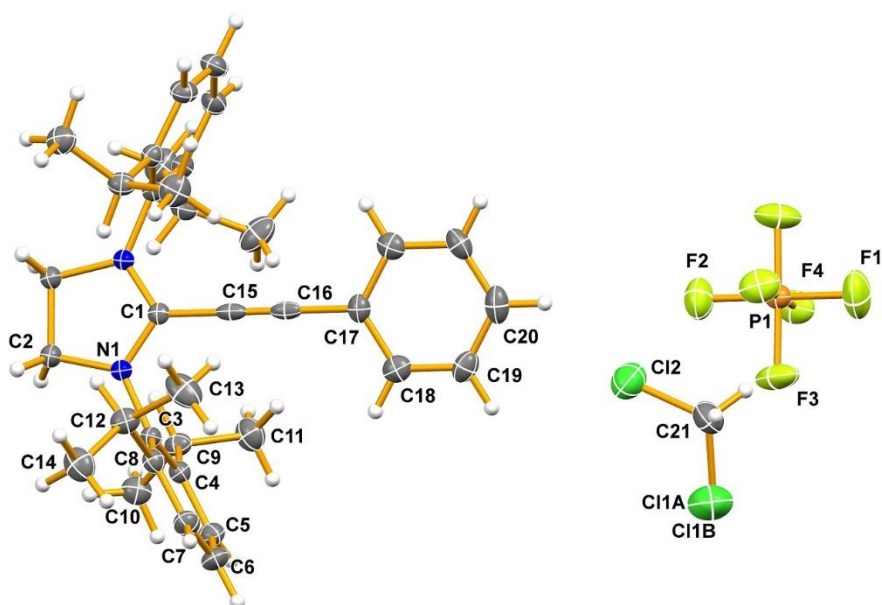


Figure S15: Solid state structure of compound **2**[PF<sub>6</sub>] with co-crystallized dichloromethane.

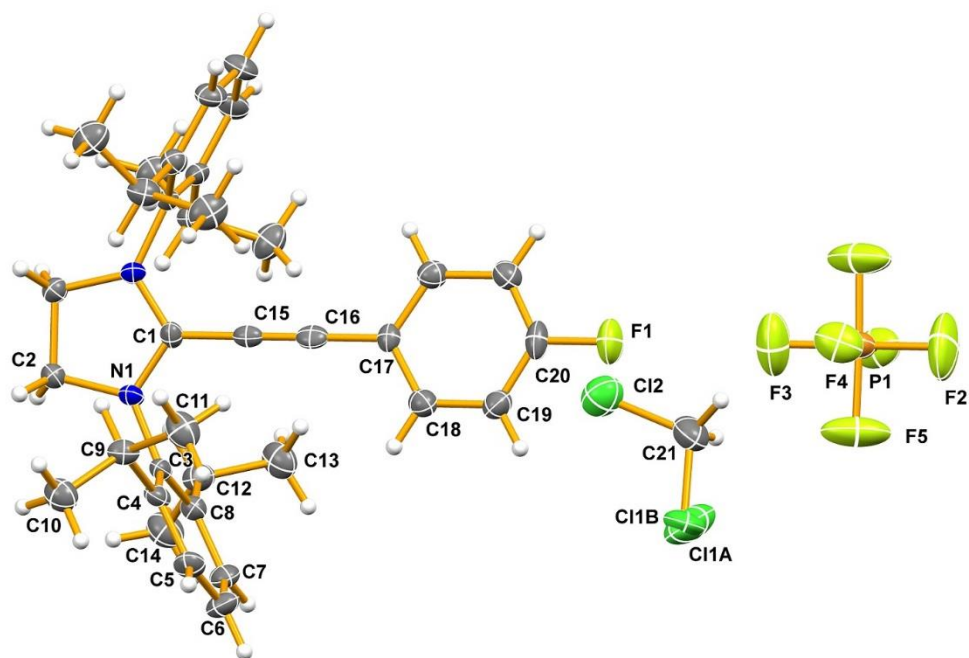


Figure S16: Solid state structure of compound *para*-F-2[PF<sub>6</sub>] with co-crystallized dichloromethane.

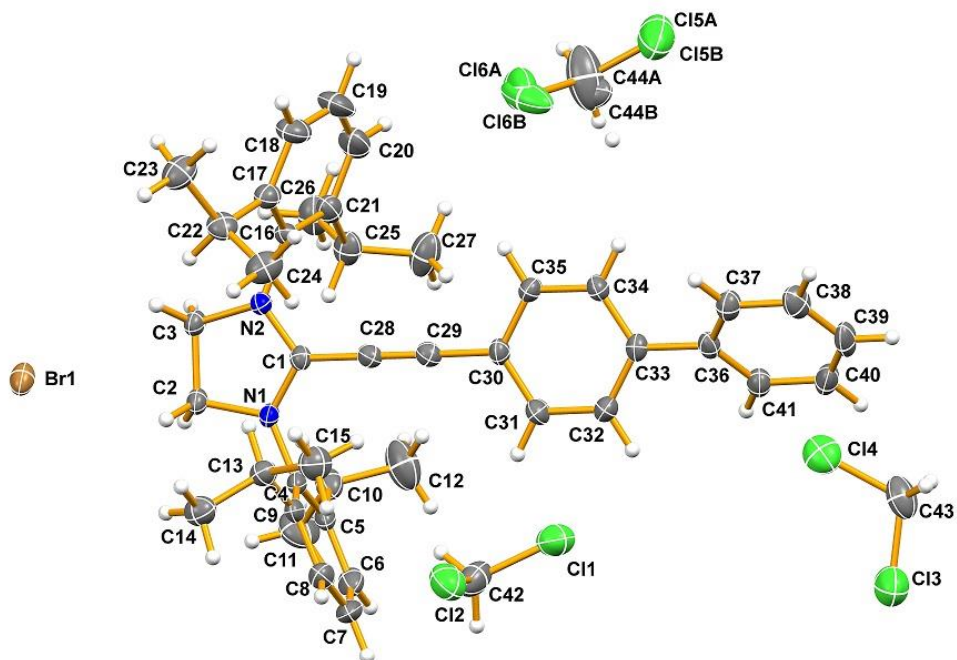
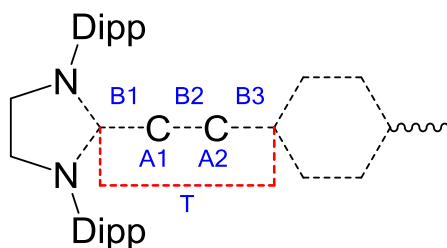


Figure S17: Solid state structure of compound *para*-Ph-2[Br] with co-crystallized dichloromethane molecules.

Table S5: Bond Lengths (Å) and Bond Angles (°) for the Central Region of Compounds **2**[Br], **3**[Br], **4**[BPh<sub>4</sub>], **5**, **2**[PF<sub>6</sub>], *para*-F-**2**[PF<sub>6</sub>], and *para*-Ph-**2**[Br]

Compound		Bond 1	Bond 2	Bond 3	Angle 1	Angle 2	Torsion
<b>5</b>		1.359(6)	1.239(6)	1.376(7)	167.0(5)	175.2(5)	-23
<b>2</b> [Br]	Molecule 1	1.424(4)	1.196(4)	1.428(4)	171.3(3)	178.4(4)	34
	Molecule 2	1.423(4)	1.203(4)	1.431(4)	167.3(3)	175.0(3)	25
<b>3</b> [Br]		1.417(4)	1.197(4)	1.430(4)	163.9(3)	176.2(3)	-17
<b>4</b> [BPh <sub>4</sub> ]		1.426(5)	1.174(4)	1.448(5)	176.0(4)	176.1(4)	136
<b>2</b> [PF <sub>6</sub> ]		1.455(4)	1.100(3)	1.472(4)	180	180	0
<i>para</i> -F- <b>2</b> [PF <sub>6</sub> ]		1.416(8)	1.184(7)	1.426(8)	180	180	0
<i>para</i> -Ph- <b>2</b> [Br]		1.424(3)	1.187(3)	1.431(3)	175.7(3)	179.4(3)	115



## References

1. (a) K. M. Kuhn, R. H. Grubbs, *Org. Lett.* **2008**, *10*, 2075–2077. (b) A. J. Arduengo III, R. Krafczyk, R. Schmutzler, H. A. Craig, J. R. Goerlich, W. J. Marshall, M. Unverzagt, M. *Tetrahedron* **1999**, *55*, 14523–14534.
2. M. Li, Y. Li, B. Zhao, F. Liang, L.-Y. Jin, *RSC Adv.* **2014**, *4*, 30046–30049.
3. N. Sun, Y. Li, G. Yin, S. Jiang, *Eur. J. Org. Chem.* **2013**, 2541–2544.
4. Gaussian 09, Revision D.1 M. J. Frisch, G. W. Trucks, H. B. Schlegel, G. E. Scuseria, M. A. Robb, J. R. Cheeseman, G. Scalmani, V. Barone, G. A. Petersson, H. Nakatsuji, X. Li, M. Caricato, A. Marenich, J. Bloino, B. G. Janesko, R. Gomperts, B. Mennucci, H. P. Hratchian, J. V. Ortiz, A. F. Izmaylov, J. L. Sonnenberg, D. Williams-Young, F. Ding, F. Lipparini, F. Egidi, J. Goings, B. Peng, A. Petrone, T. Henderson, D. Ranasinghe, V. G. Zakrzewski, J. Gao, N. Rega, G. Zheng, W. Liang, M. Hada, M. Ehara, K. Toyota, R. Fukuda, J. Hasegawa, M. Ishida, T. Nakajima, Y. Honda, O. Kitao, H. Nakai, T. Vreven, K. Throssell, J. A. Montgomery, Jr., J. E. Peralta, F. Ogliaro, M. Bearpark, J. J. Heyd, E. Brothers, K. N. Kudin, V. N. Staroverov, T. Keith, R. Kobayashi, J. Normand, K. Raghavachari, A. Rendell, J. C. Burant, S. S. Iyengar, J. Tomasi, M. Cossi, J. M. Millam, M. Klene, C. Adamo, R. Cammi, J. W. Ochterski, R. L. Martin, K. Morokuma, O. Farkas, J. B. Foresman, and D. J. Fox, Gaussian, Inc., Wallingford CT, 2009.
5. (a) J. P. Perdew, K. Burke, M. Ernzerhof, *Phys. Rev. Lett.* **1996**, *77*, 3865–3868. (b) J. P. Perdew, K. Burke, M. Ernzerhof, *Phys. Rev. Lett.* **1997**, *78*, 1396–1396. (c) J. P. Perdew, M. Ernzerhof, K. Burke, *J. Chem. Phys.* **1996**, *105*, 9982–9985. (d) C. Adamo, V. Barone, *J. Chem. Phys.* **1999**, *110*, 6155–6159.
6. F. Weigend, R. Ahlrichs, *Phys. Chem. Chem. Phys.* **2005**, *7*, 3297–3305.
7. A. Schäfer, C. Huber, R. Ahlrichs, *J. Chem. Phys.* **1994**, *100*, 5829–5835.
8. K. Wolinski, J.F. Hilton, P. Pulay, *J. Am. Chem. Soc.* **1990**, *112*, 8251–8260.
9. (a) C. Corminboeuf, T. Heine, G. Seifert, P. v. R. Schleyer, J. Weber, *Phys. Chem. Chem. Phys.* **2004**, *6*, 273–276. (b) H. Fallah-Bagher-Shaidaei, C. S. Wannere, C. Corminboeuf, R. Puchta, P. v. R. Schleyer, *Org. Lett.* **2006**, *8*, 863–866.
10. R. E. Stratmann, G. E. Scuseria, M. J. Frisch, *J. Chem. Phys.* **1998**, *109*, 8218–8224.
11. J. Tomasi, B. Mennucci, R. Cammi, *Chem. Rev.* **2005**, *105*, 2999–3093.
12. R. G. Compton, C. E. Banks, *Understanding Voltammetry*, Imperial College Press, London, **2011**, p. 429.
13. APEX2, Bruker AXS Inc., 2008, Madison, Wisconsin, USA.
14. SAINT, Bruker AXS Inc., 2008, Madison, Wisconsin, USA.
15. SADABS, Bruker AXS Inc., 2009, Madison, Wisconsin, USA.
16. L. Palatinus, G. Chapuis, *J. Appl. Crystallogr.* **2007**, *40*, 786–790.
17. I. Palatinus, S. J. Prathapa, S. van Smaalen, *J. Appl. Crystallogr.* **2012**, *45*, 575–580.
18. (a) G. M. Sheldrick, *Acta Cryst.* **2008**, *A64*, 112–122. (b) G. M. Sheldrick, *Acta Cryst.* **2015**, *A71*, 3–8.
19. G. M. Sheldrick, *Acta Cryst.* **2015**, *C71*, 3–8.